

**Atmospheric Turbulence Aircraft Measurement Data
Report and Raw Data Summary:**

Final Report 2006

Analysis of 2006 EGRETT Data: 060809

Prepared by:

Donald Wroblewski, DEW Consulting

Prepared for:

Jorg Hacker, Airborne Research Australia

Owen Cote: Air Force Research Laboratory

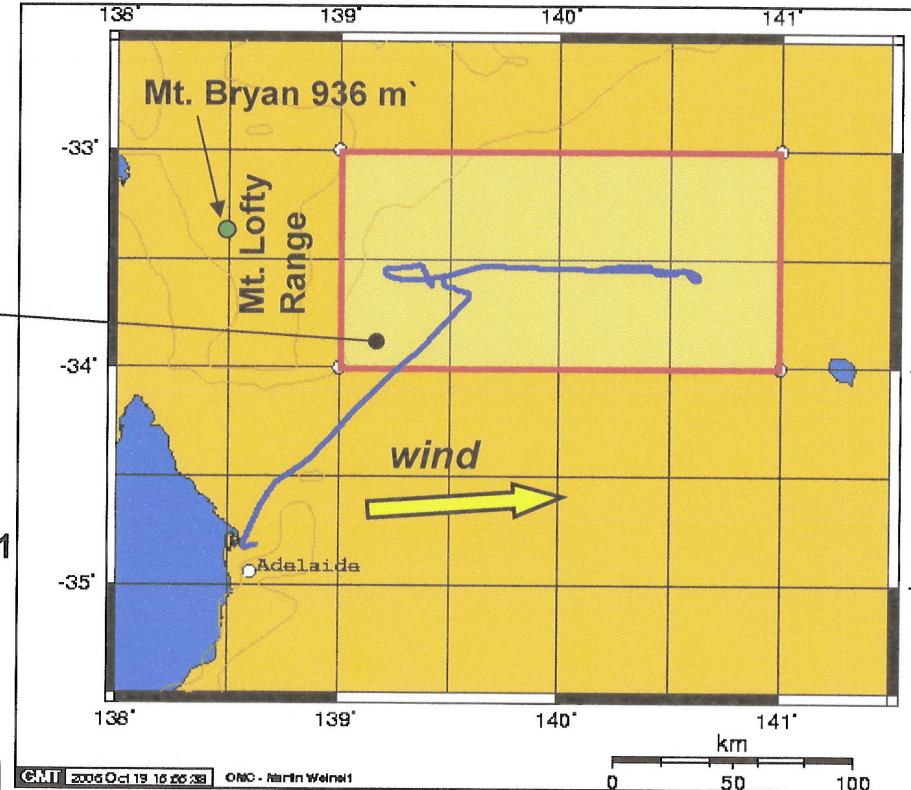
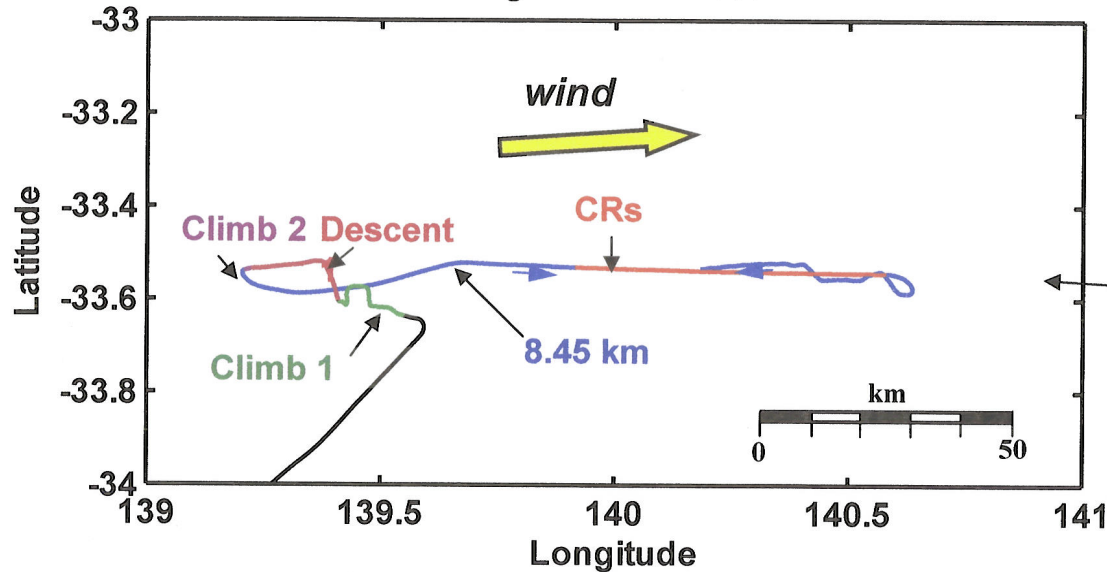
Report Documentation Page			Form Approved OMB No. 0704-0188		
Public reporting burden for the collection of information is estimated to average 1 hour per response, including the time for reviewing instructions, searching existing data sources, gathering and maintaining the data needed, and completing and reviewing the collection of information. Send comments regarding this burden estimate or any other aspect of this collection of information, including suggestions for reducing this burden, to Washington Headquarters Services, Directorate for Information Operations and Reports, 1215 Jefferson Davis Highway, Suite 1204, Arlington VA 22202-4302. Respondents should be aware that notwithstanding any other provision of law, no person shall be subject to a penalty for failing to comply with a collection of information if it does not display a currently valid OMB control number.					
1. REPORT DATE 04 JAN 2007		2. REPORT TYPE		3. DATES COVERED	
4. TITLE AND SUBTITLE Atmospheric Turbulence Aircraft Measurement Data Report and Raw Data Summary				5a. CONTRACT NUMBER FA48690610083	
				5b. GRANT NUMBER	
				5c. PROGRAM ELEMENT NUMBER	
6. AUTHOR(S) Jorg Hacker				5d. PROJECT NUMBER	
				5e. TASK NUMBER	
				5f. WORK UNIT NUMBER	
7. PERFORMING ORGANIZATION NAME(S) AND ADDRESS(ES) ARA-Airborne Research Australia Pty Ltd,PO Box 335,Salisbury South 5106,AU,5106				8. PERFORMING ORGANIZATION REPORT NUMBER N/A	
9. SPONSORING/MONITORING AGENCY NAME(S) AND ADDRESS(ES)				10. SPONSOR/MONITOR'S ACRONYM(S)	
				11. SPONSOR/MONITOR'S REPORT NUMBER(S)	
12. DISTRIBUTION/AVAILABILITY STATEMENT Approved for public release; distribution unlimited.					
13. SUPPLEMENTARY NOTES					
14. ABSTRACT This report describes a data analysis effort to understand high-altitude turbulence measurements made on an EGRETT aircraft flown in Southern Australia.					
15. SUBJECT TERMS					
16. SECURITY CLASSIFICATION OF:			17. LIMITATION OF ABSTRACT	18. NUMBER OF PAGES 34	19a. NAME OF RESPONSIBLE PERSON
a. REPORT unclassified	b. ABSTRACT unclassified	c. THIS PAGE unclassified			

Outline/Table of Contents 060809 Data Analysis

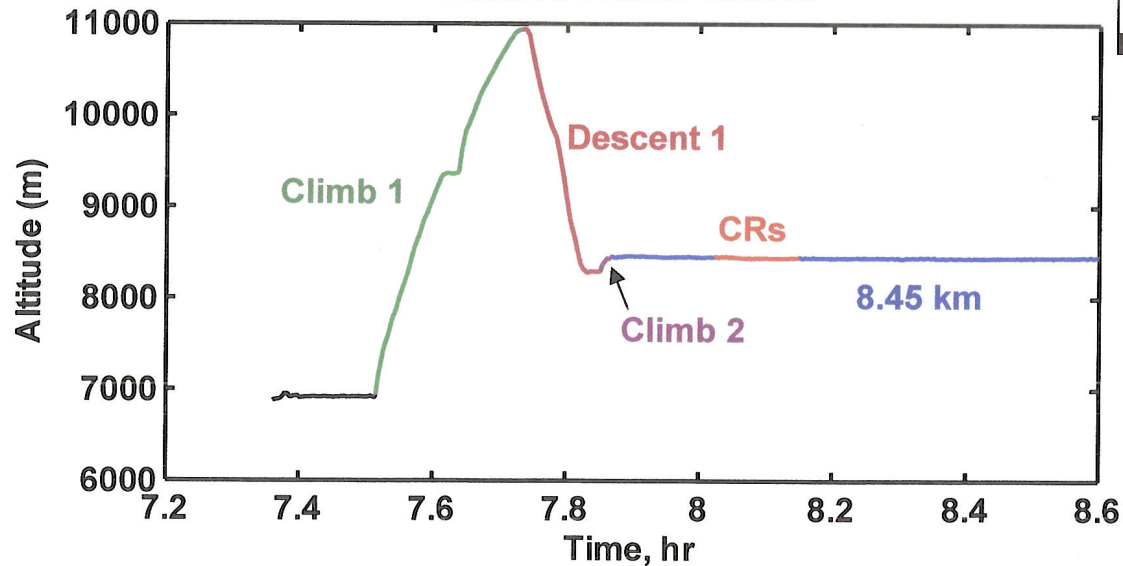
- Flight Paths [slide 3](#)
- Vertical gradients [slides 4 5](#)
- Ramp Offs in W 18.45 km level:
 - Identification [slides 6 9](#)
 - Vertical depth estimate [slide 10](#)
 - Velocity and temperature correlations [slides 14 5](#)
 - Explanations for positive vertical heat flux [slides 16 19](#)
 - Structure functions and spectra [slides 20 24](#)
 - Structure constants and length scales [slides 25 28](#)
- Cliff ramps in E 18.45 km level:
 - Identification [slides 27 28](#)
 - Velocity and temperature correlations [slides 29 30](#)
 - Structure functions, spectra and length scales [slide 31 32](#)
- Summary [slides 33 34](#)

FLIGHT PATHS: 060809

Flight Path 060809

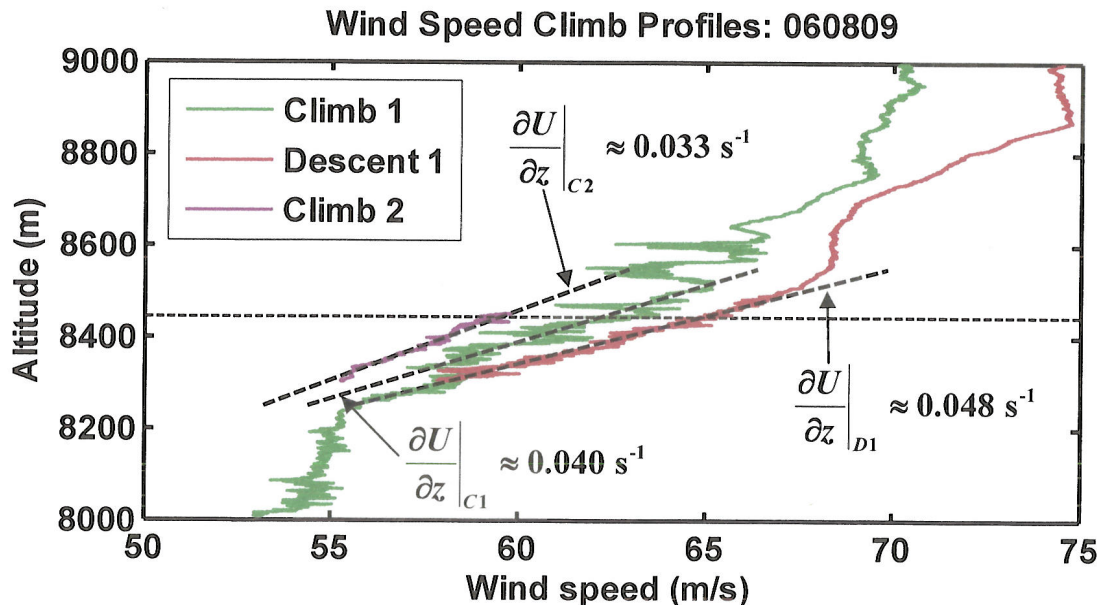
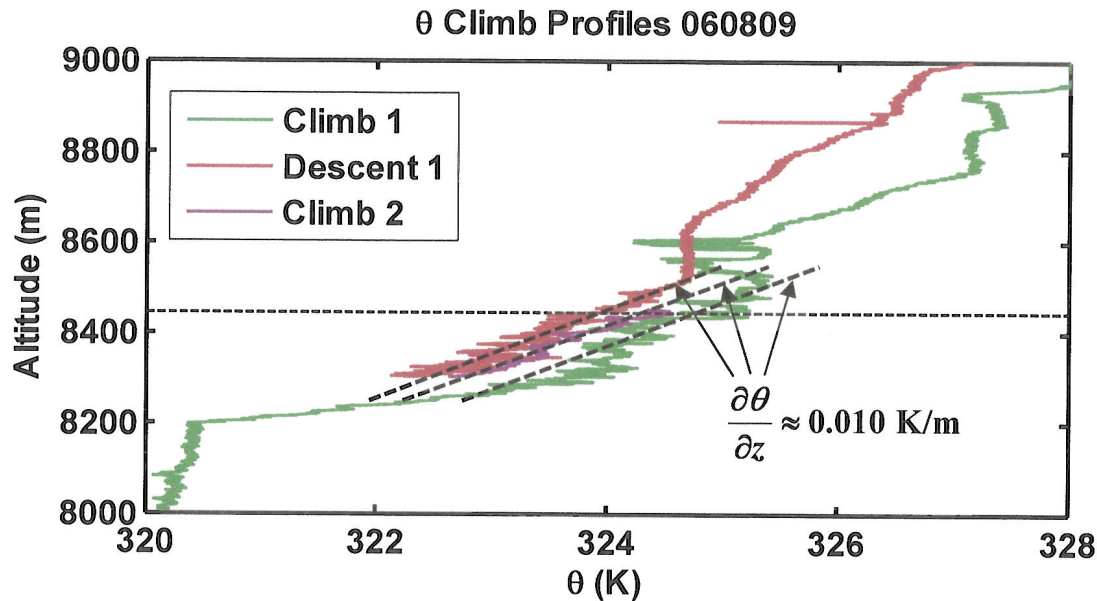


Altitude Profile: 060809



- Main level segment at 8.45 km is 100 to 200 km downwind of Mt. Lofty range, including Mt. Bryan (960 m)
- Difference between wind and flight directions only 7°.

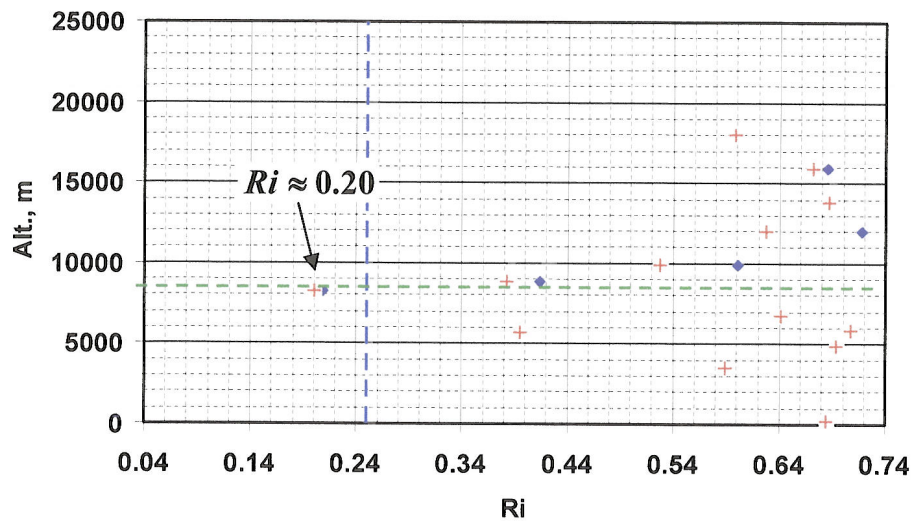
CLIMB/DESCENT DATA AND GRADIENT ESTIMATES



- Gradients found by fitting data from climb/descent segments around 8.45 km level (horizontal dashed line).
- Fluctuations in θ and U suggest layer is between 8.26 and 8.61 km (350 m thick).
- Negligible gradients in wind direction (not shown): no directional shear.
- Same $d\theta/dz$ gradient for all three climb/descent segments, but different shear.
- Ri number estimate

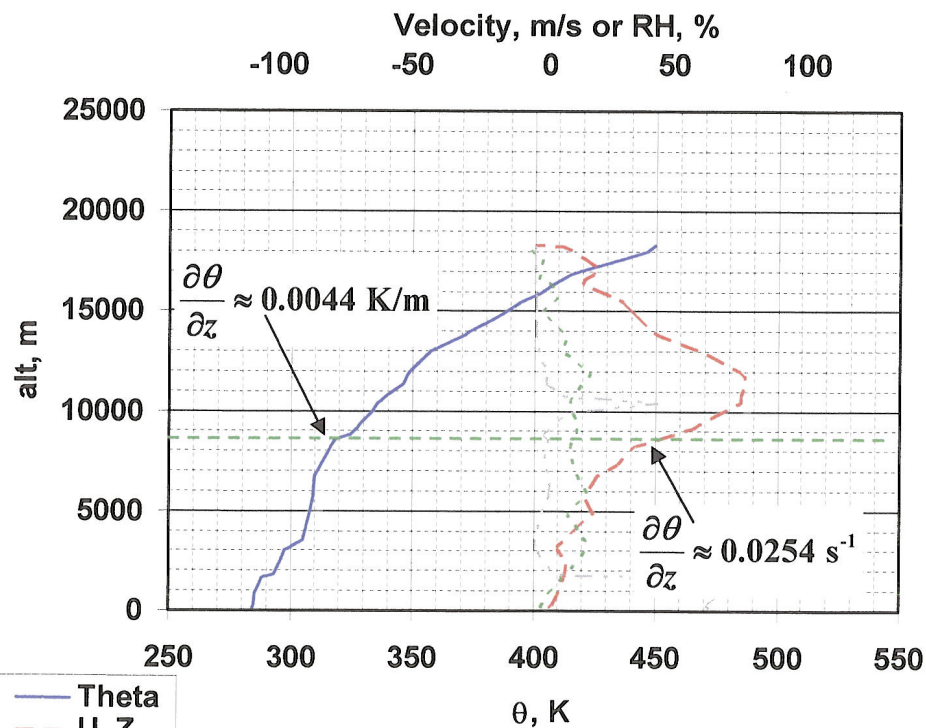
	$S_z \text{ (s}^{-1}\text{)}$	$N_z \text{ (s}^{-1}\text{)}$	Ri
Climb1	0.040	0.018	0.20
Descent	0.048	0.018	0.14
Climb 2	0.033	0.018	0.30
AVE:	0.040	0.018	0.20

SOUNDINGS: ADELAIDE 00Z Aug. 9, 2006



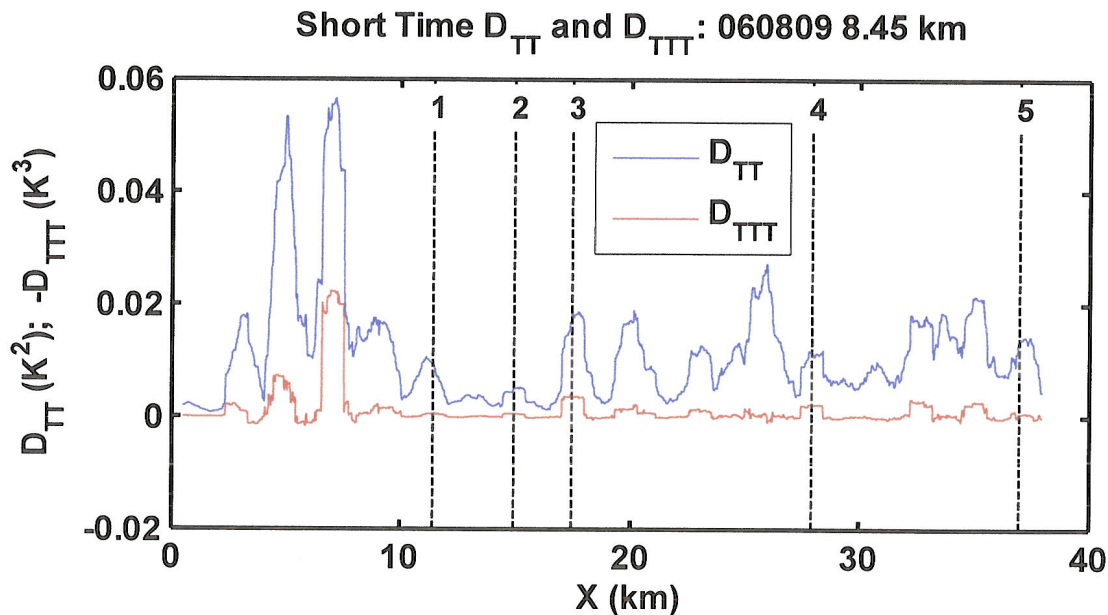
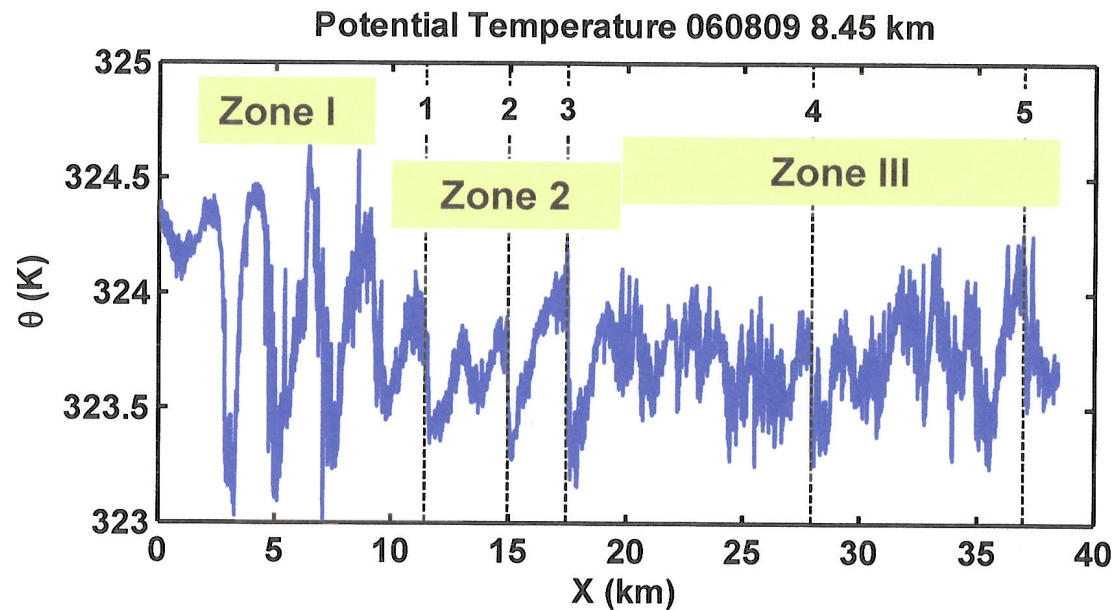
- Soundings predict layer between 8,260 m and 8,607 m (344 m thick)- very close to what climb data shows.

- θ and U gradients from soundings are both low compared to those from climb data, though resulting Richardson number (0.20) is the same as the average of the three values found from the climb segments.



— Theta
-- U_Z
... U_M
- . RH

POTENTIAL TEMPERATURE & SHORT TIME D_{TT} & D_{TTT}

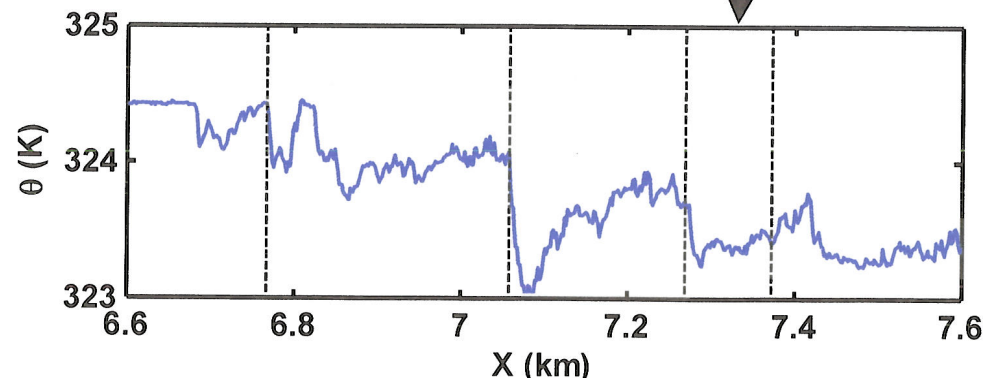
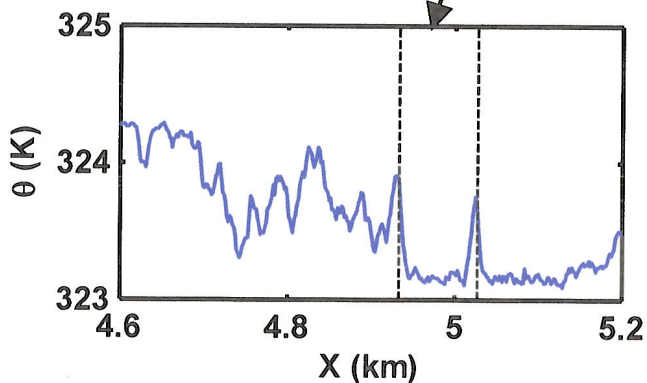
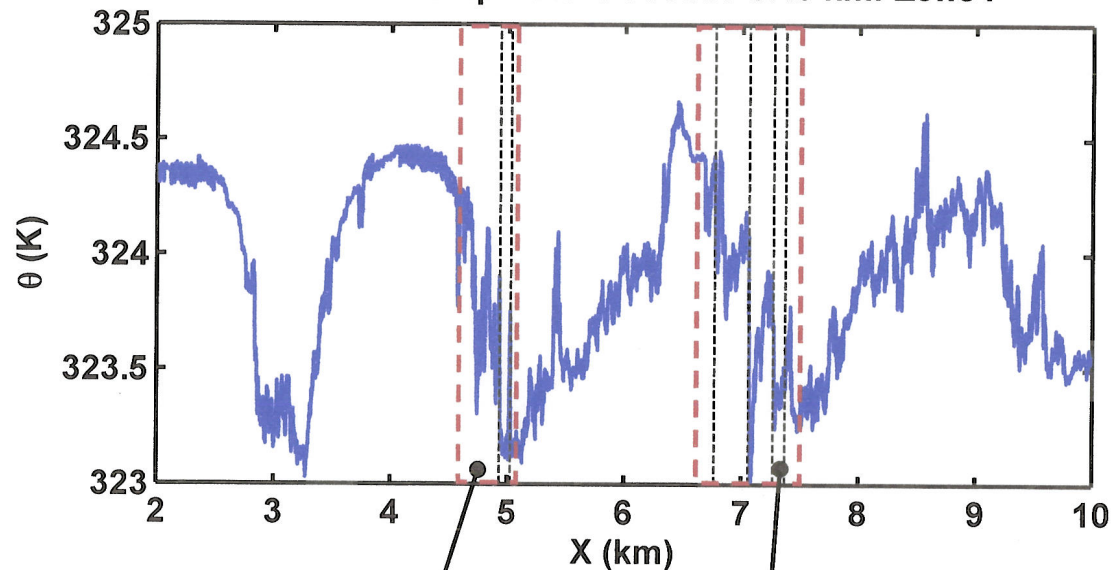


- 3 distinct regions.
 - I. 2-10 km: nearly symmetric, wave-like features, with large small scale fluctuations.
 - II. 10-18 km: 3 ramp-cliffs (marked), with similar wavelengths, but smaller amplitudes than the wave-like features in zone I.
 - III. >18 km: Mixture of symmetric structures and RC's and increased smaller-scale turbulence.

Unlike other CR cases studied, the highest D_{TTT} values are not at the three cliffs, but are associated with fluctuations during the wave-like features in Zone I. (See slide 7)

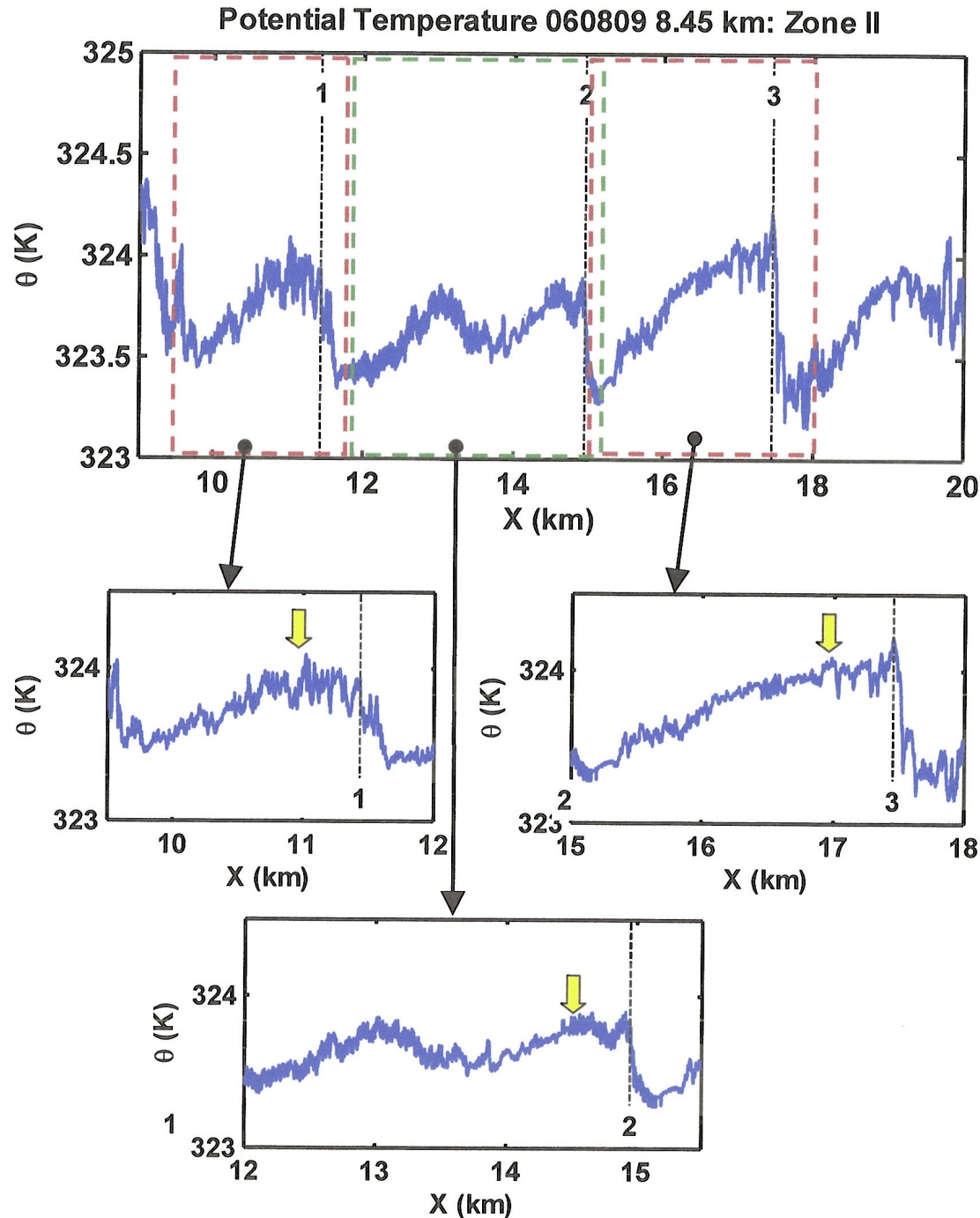
ZONE I: POTENTIAL TEMPERATURE

Potential Temperature 060809 8.45 km: Zone I



- Structures start out with finger-like shapes (2-5 km), and then become symmetric ramps without cliffs (5-10).
- High values of D_{TT} and D_{TTT} are associated with small-scale features (vertical lines) seen during decreasing temperature phase of first 2 large-scale structures.
- First 2 (middle plot) are only ≈ 30 m wide and appear symmetric. The large negative D_{TTT} values are due to steep gradients just after the peak temperature.
- Large D_{TTT} values for second large-scale structure is mainly due to 200 m wide ramp-cliff at 7 km, but several other similarly sized ramp-cliffs (30 to 200 m wide) are also evident (marked by vertical lines)

ZONE II: POTENTIAL TEMPERATURE



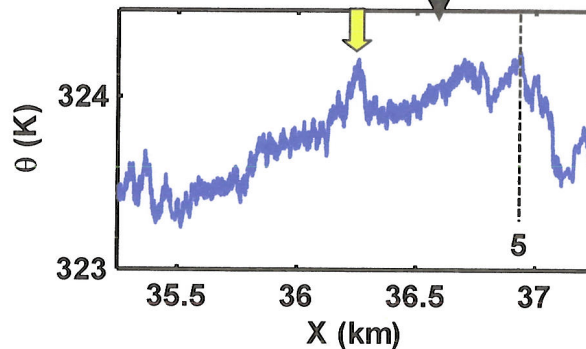
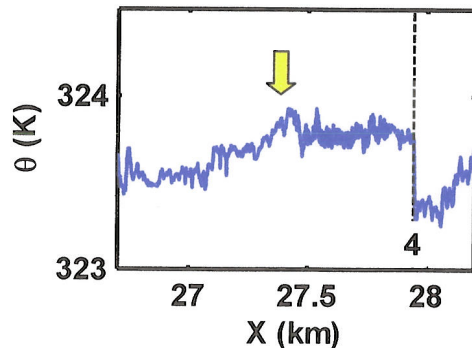
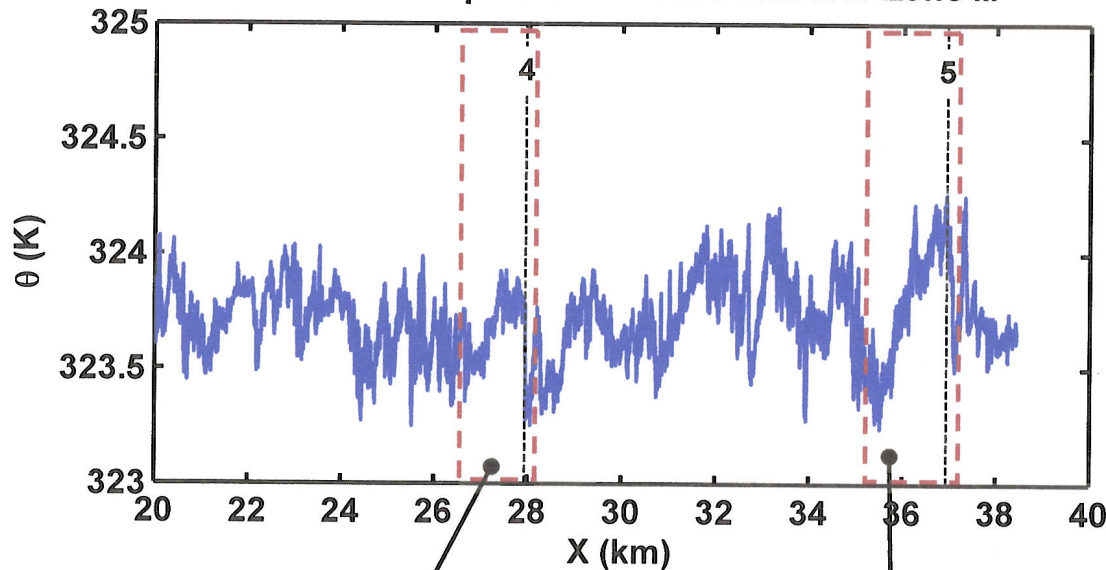
- 3 ramp-cliffs (RC consistent with tailwind and positive shear).

	Cliff width (m)	Wavelength (km)	$\Delta\theta$ (K)
1.	210	1.86	0.55
2.	200	1.54	0.50
3.	79	2.38	0.87
AVE.	163	1.90	0.64

- These are weak RC's ($\Delta\theta$ from 0.5 to 0.87 K), with broad weak cliffs for the first two RC's.
- Symmetric feature with a similar wavelength (1.9 km) is seen between RCs 1& 2.
- All ramps have distinct shape, featuring a plateau with increased fluctuations before cliff (yellow arrows). Is this due to vertical location in billow?

ZONE III: POTENTIAL TEMPERATURE

Potential Temperature 060809 8.45 km: Zone III



- 2 more ramp-cliffs

	Cliff width (m)	Wavelength (km)	$\Delta\theta$ (K)
4.	17	1.11	0.47
5.	221	1.65	0.75
AVE*	145	1.69	0.63

***AVERAGES FOR ALL 5 RC's**

- RC 5 is similar to the RC's in Zone III.
- RC 4 has the steepest cliff of all five RCs, 17 m wide only 1.5 % of the total wavelength of RC. This is smaller than all but 1 of the RC/CRs observed in all campaigns.
- Ramps of RC 4 exhibits plateau before cliff, similar to RCs in Zone I.
- "Disturbance" seen in middle of both ramp for both RC 5 and 6. (yellow arrows).

LAYER DEPTH ESTIMATE

	$\Delta\theta_{CLIFF}$ (K)	H (m)	L (m)	AR = L/H
RC 1	0.55	55	1,860	33
RC 2	0.50	50	1,540	31
RC 3	0.87	87	2,380	28
RC 4	0.47	47	1,100	23
RC 5	0.75	75	1,650	22
AVE	0.63	63	1,700	27

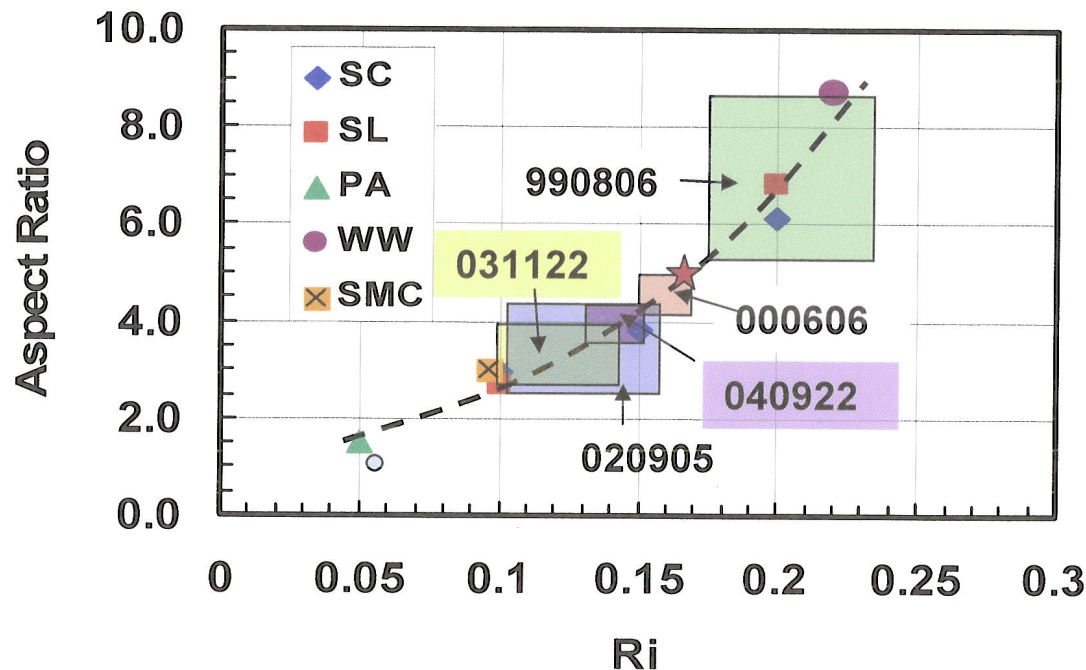
$$H \approx \Delta\theta_{CLIFF} / \frac{\partial\theta}{\partial z}$$

See slide 26, 2005 Briefing 1 for details

$$\frac{\partial\theta}{\partial z} = 0.01 \text{ K/m}$$

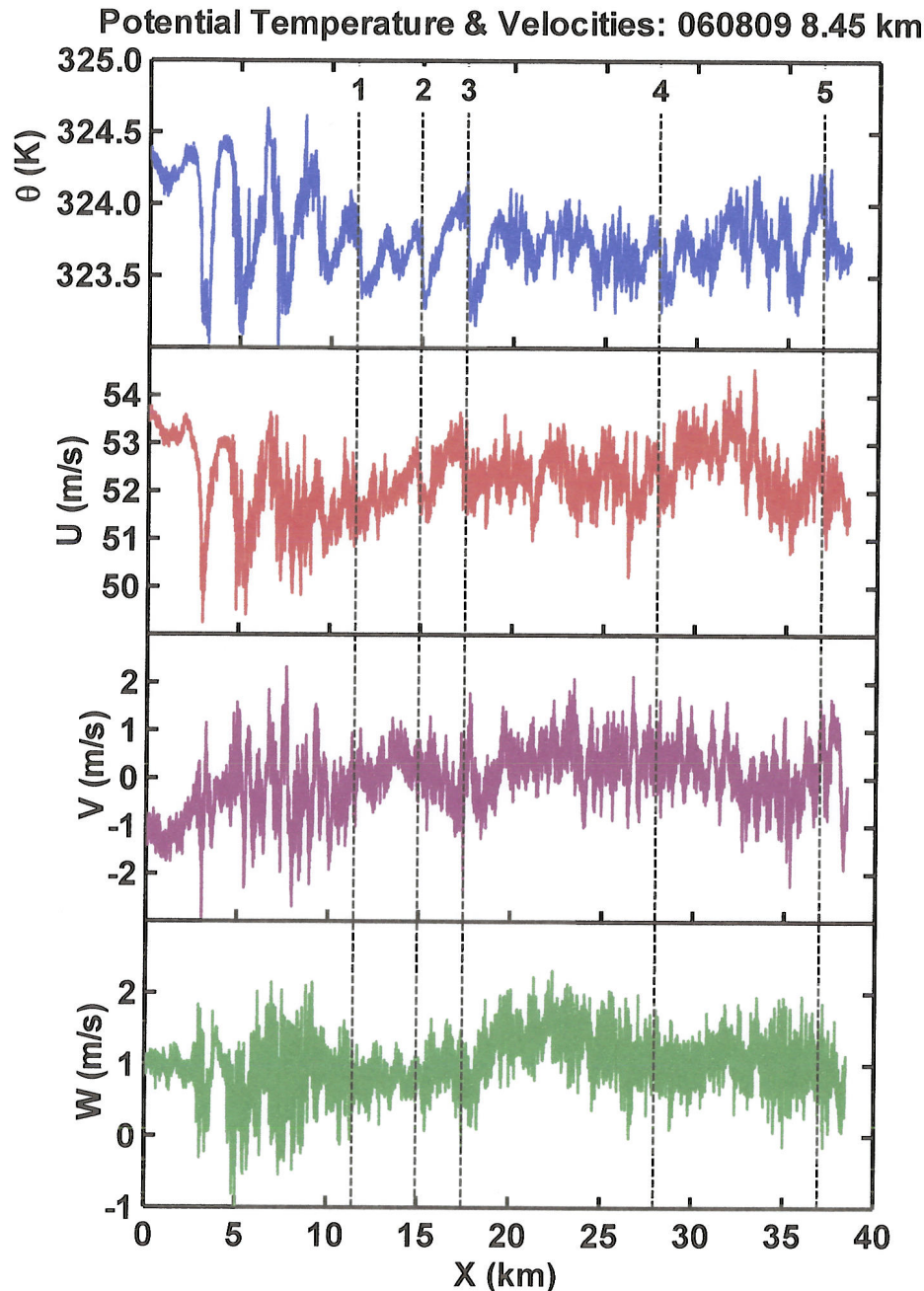
- The extremely low value for the aspect ratio is out of line with values from other CR/RC's and DNS, as seen in plot (see slide 35, 2005 Briefing 3 for key to DNS)
- However, the climb data (slide 4) and soundings (slide 5) suggest a layer that is 350 m deep, which corresponds to an aspect ratio of 4.9 (red star in plot) which is consistent with the previously observed CRs and an initial Ri of around 0.17.

Aspect ratio vs. Richardson No. for DNS



Why is the estimate incorrect? Is $d\theta/dz$ too high? or maybe the aircraft is flying near top of layer where $\Delta\theta$ is smaller. (Will check latter with J. Werne's DNS).

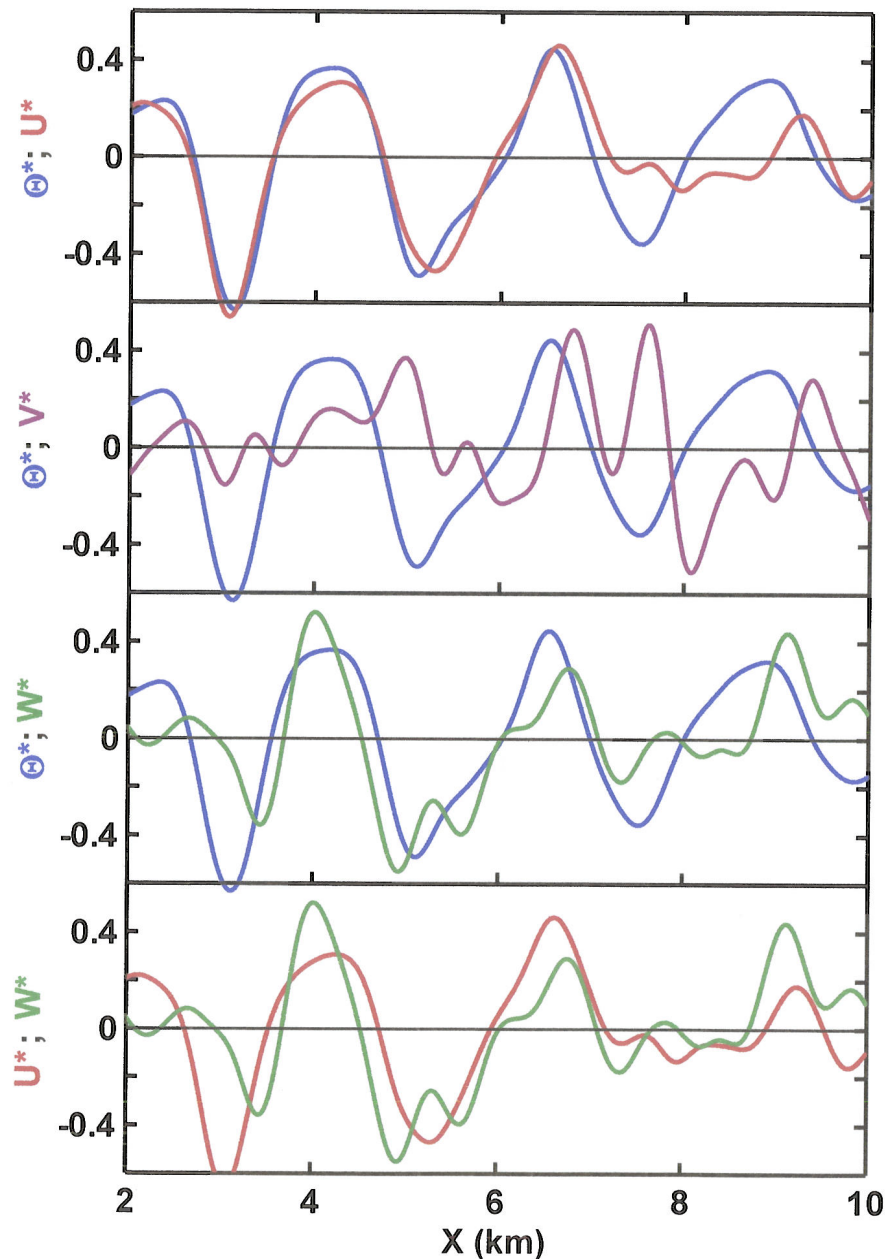
TEMPERATURE & VELOCITIES: ALL ZONES



- U (velocity in mean wind direction) displays large-scale features very similar to θ .
- Pattern of small-scale turbulence best seen in W signal- large in Zone I, decreasing in Zone II and increasing again in Zone III.
 - This behavior is different than previously analyzed RC/CRs (see previous ARA briefings), which showed increased smaller-scale turbulence when RC/CRs arose.

FILTERED & NORMALIZED TEMP. & VELOCITIES: ZONE I

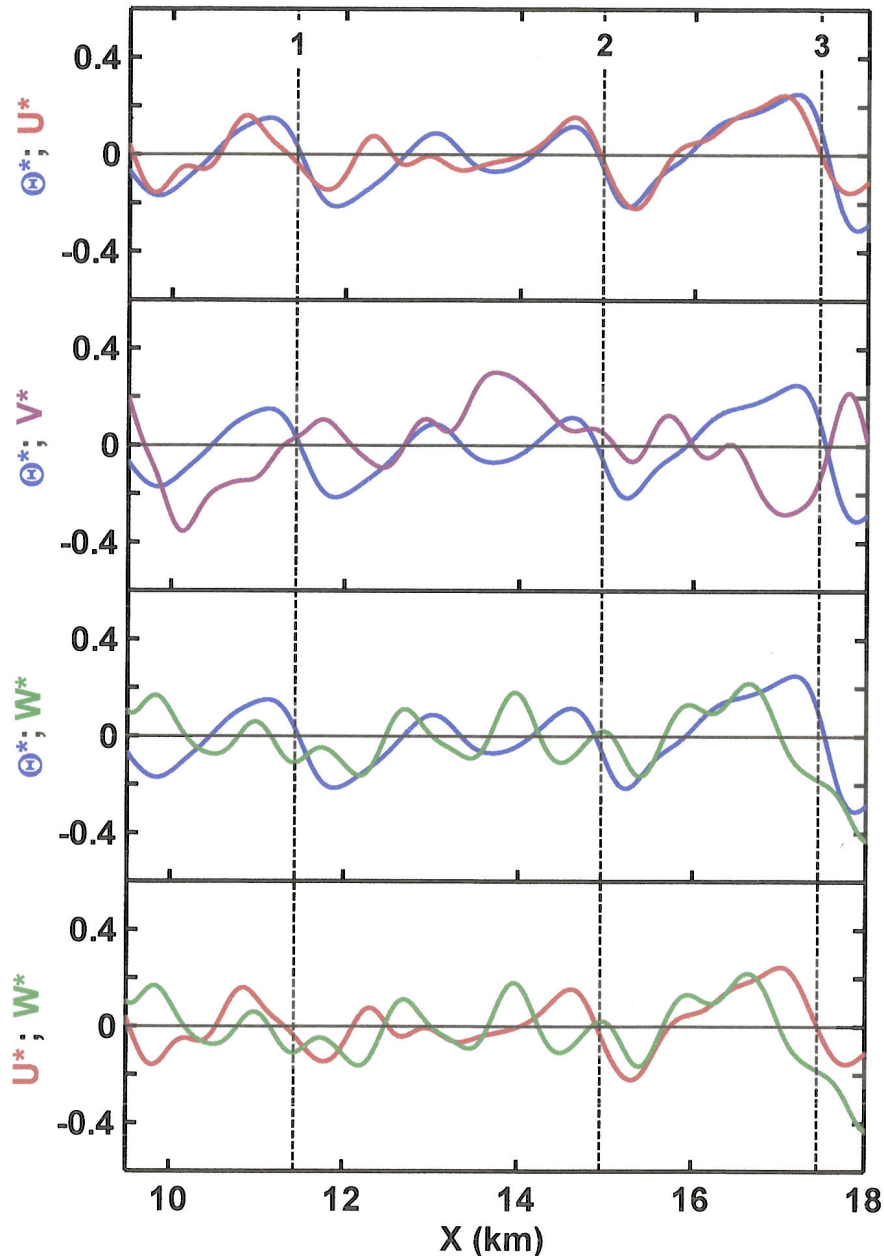
Normalized Filtered U, V, W, θ : 060809 8.45 km, Zone I



- Velocity and temperature bandpass filtered with a pass band of 0.75 km to 10 km. Filtered signals were then normalized to provide non-dimensional functions with similar amplitudes.
 $X^* = x/\Delta X^*$: $\Delta\theta^* = 1.3$ K, $\Delta U^* = 2.8$ m/s, $\Delta V^* = 1.9$ m/s, $\Delta W^* = 1$ m/s.
- Wavelike features in Zone I show close correlation between θ^* and U^* , but not between V^* and θ^* .
- θ^* and W^* are also well correlated and appear to be nearly in phase for the first two structures. Similarly behavior for U^* and W^* .
- This suggests that these are not gravity waves, which would feature quadrature between θ^* and W^* .
- There is little correlation between θ^* and V^* .

FILTERED & NORMALIZED TEMP. & VELOCITIES: ZONE II

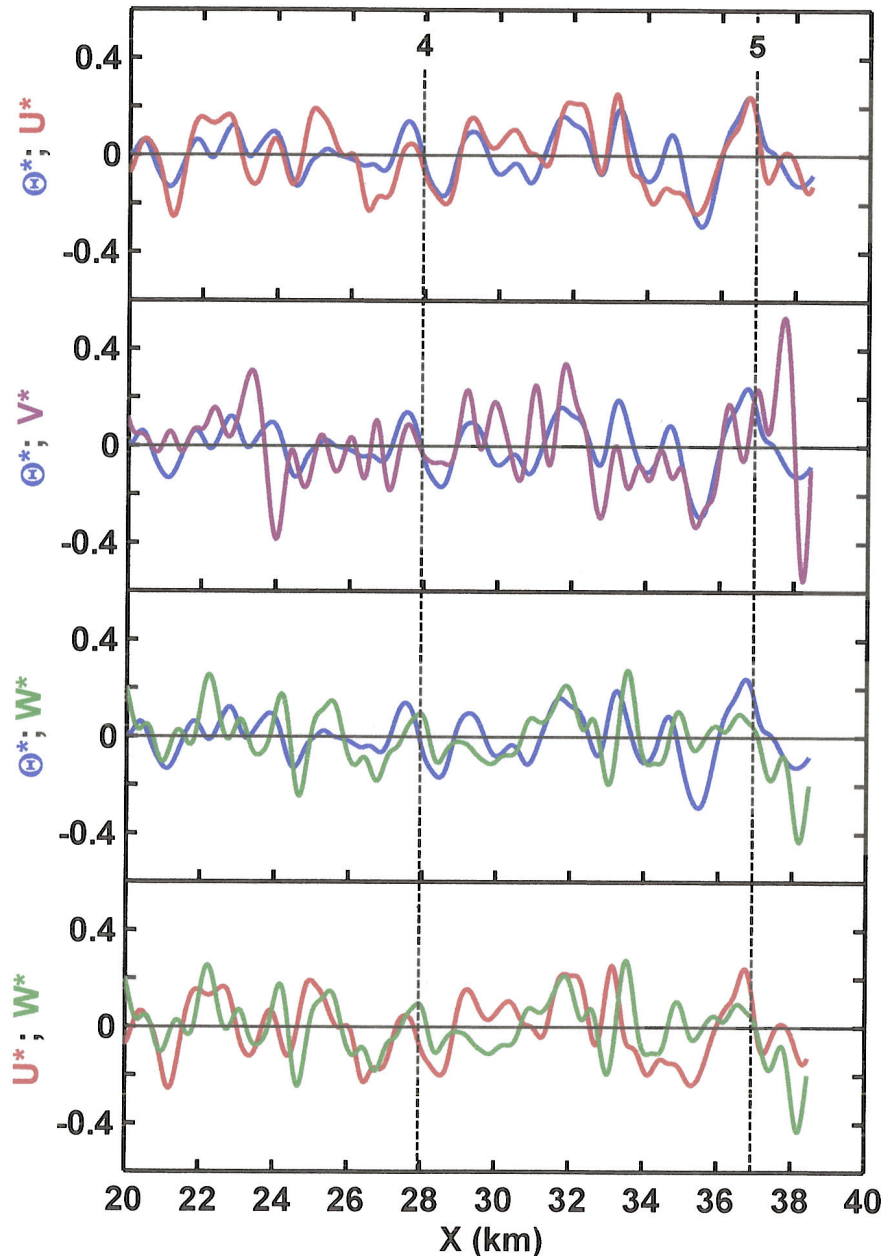
Normalized Filtered U, V, W, θ : 060809 8.45 km, Zone II



- Ramp-cliffs in Zone II show close correlation between θ^* and U^* .
- For 1st and 3rd cliff, V^* is close to 180° out of phase with θ^* .
- W^* generally decreasing prior to cliffs, with a zero crossing at the cliffs. The third cliff shows the strongest correlation between W^* and θ^* .

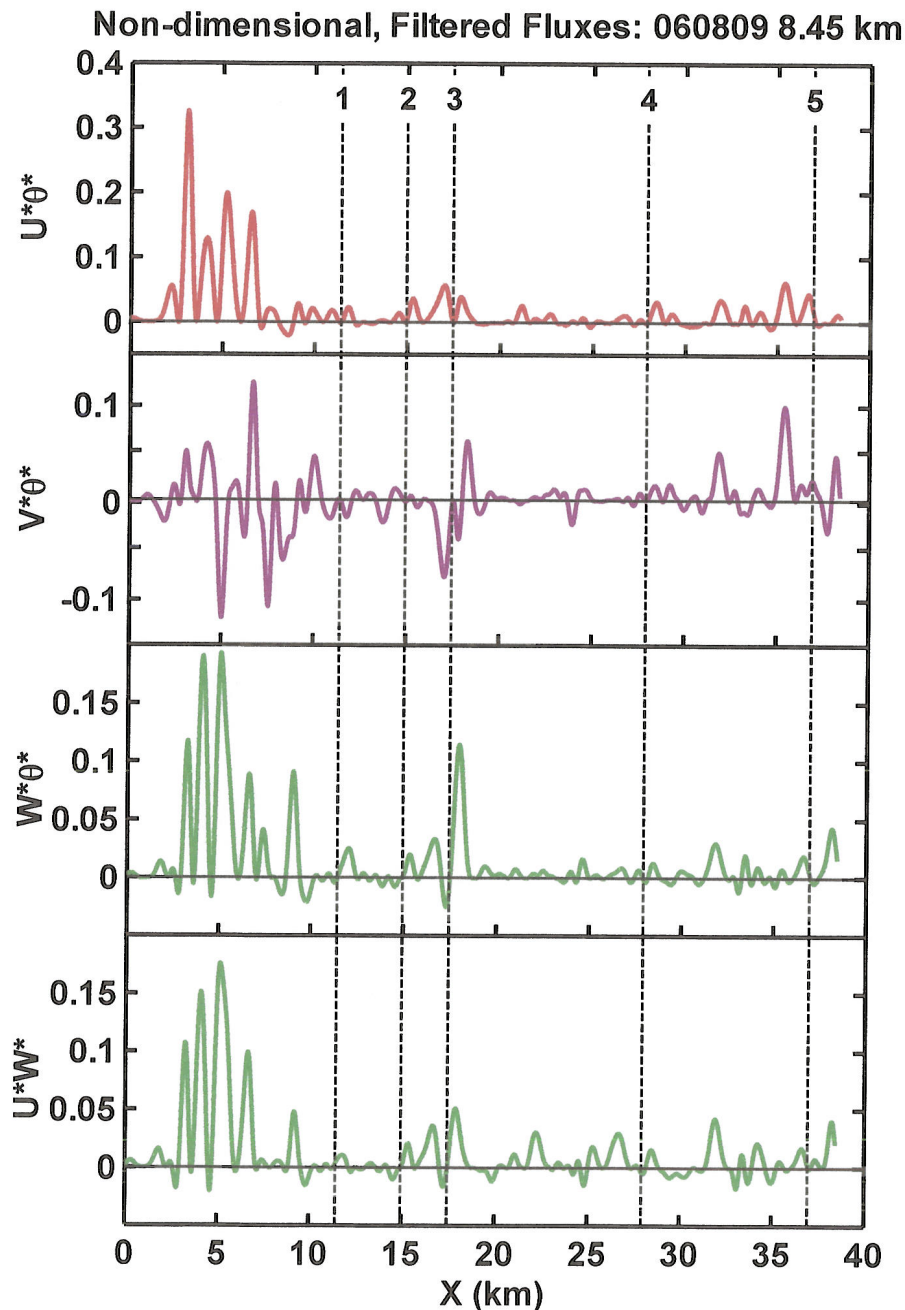
FILTERED & NORMALIZED TEMP. & VELOCITIES: ZONE III

Normalized Filtered U, V, W, θ : 060809 8.45 km, Zone III



- Close correlation between θ^* and U^* for cliff-ramps and the symmetric structures.
- Zone III features better correlation between θ^* and V^* than Zone I or II.
- W^* behavior near cliff 5 is similar to that near cliff 1 and 3 in Zone I. But near cliff 4, it is slightly different, with increasing W^* prior to the cliff.

FILTERED & NORMALIZED FLUXES: ALL ZONES



Correlation Coefficients

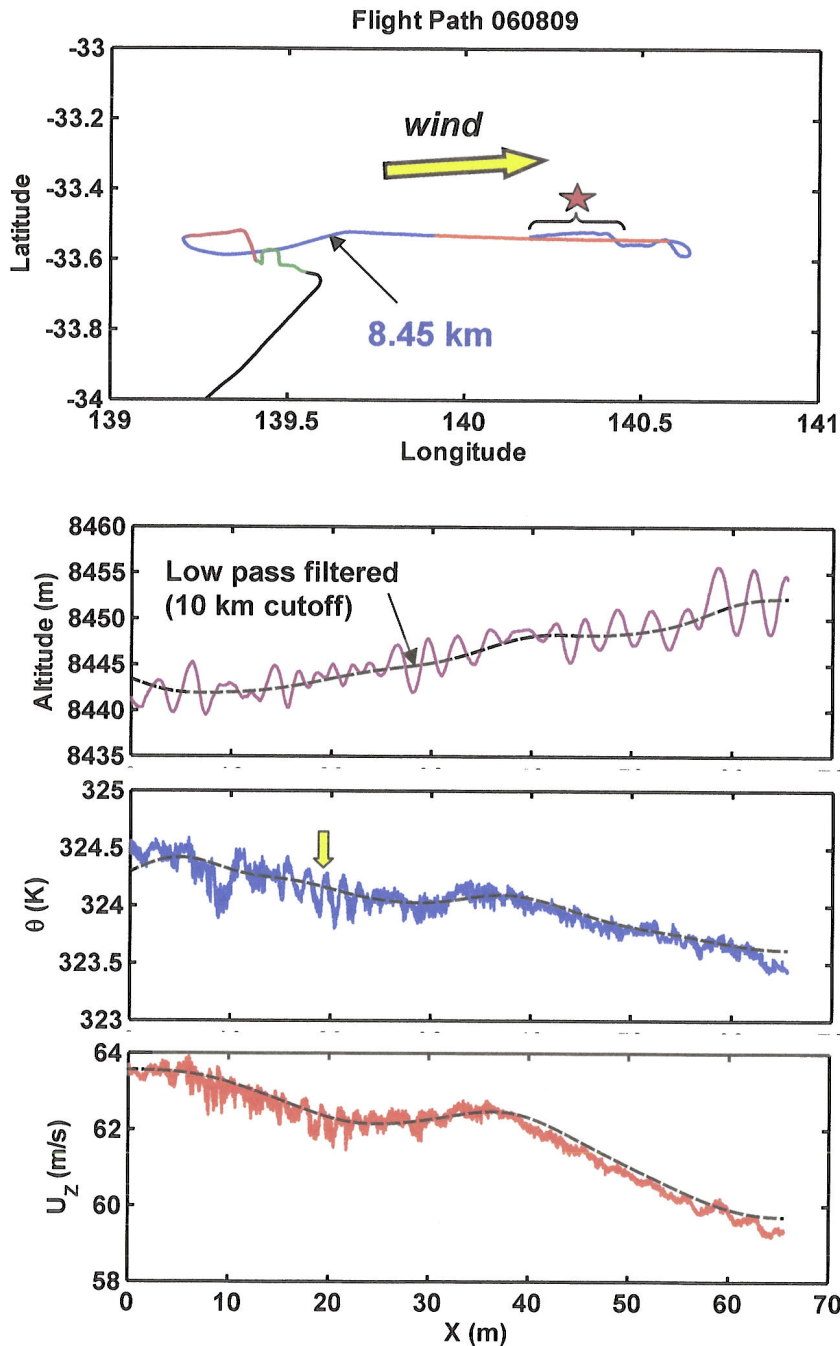
$$R_{X^*Y^*} = \frac{\langle X^*Y^* \rangle}{\sigma_{X^*}\sigma_{Y^*}}$$

	$R_{U^*\Theta^*}$	$R_{V^*\Theta^*}$	$R_{W^*\Theta^*}$	$R_{U^*W^*}$
Zone I	0.863	-0.075	0.710	0.701
Zone II	0.830	-0.169	0.529	0.419
Zone III	0.750	0.442	0.456	0.446
ALL	0.813	0.042	0.624	0.576

- $U^*\Theta^* > 0$ for almost the entire time, with high correlation coefficients (highest in Zone I.)
- In Zone III, mostly positive values of $R_{V^*\Theta^*}$.
- $W^*\Theta^*$ and U^*W^* mostly positive-- unexpected for stable stratification and positive shear. Magnitudes of $R_{W^*\Theta^*}$ are much higher than values found for other cliff ramps (990806, etc), which exhibit $R_{W^*\Theta^*}$ around -0.2
- If the small scale motions are included (i.e., high pass filtered data) the correlation coefficients are still positive.

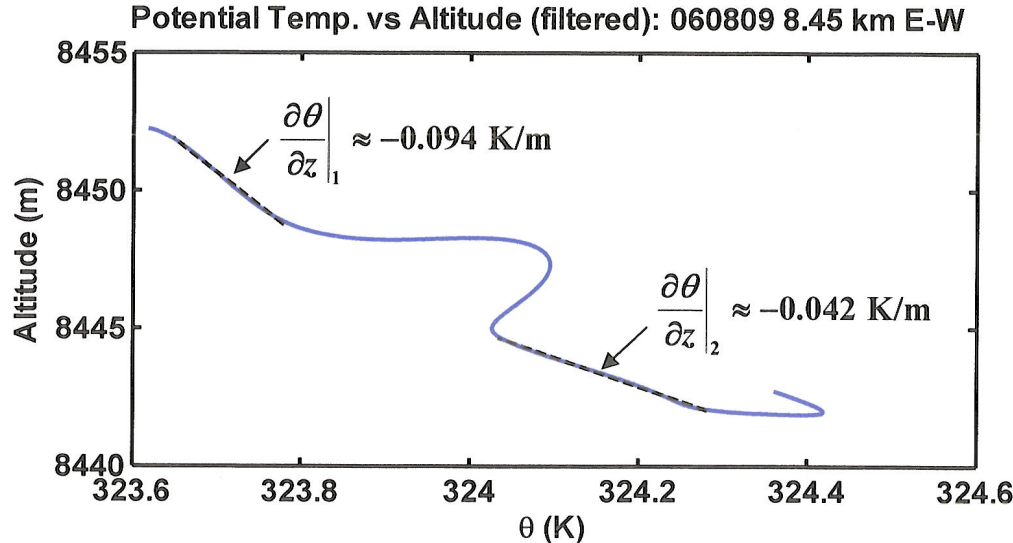
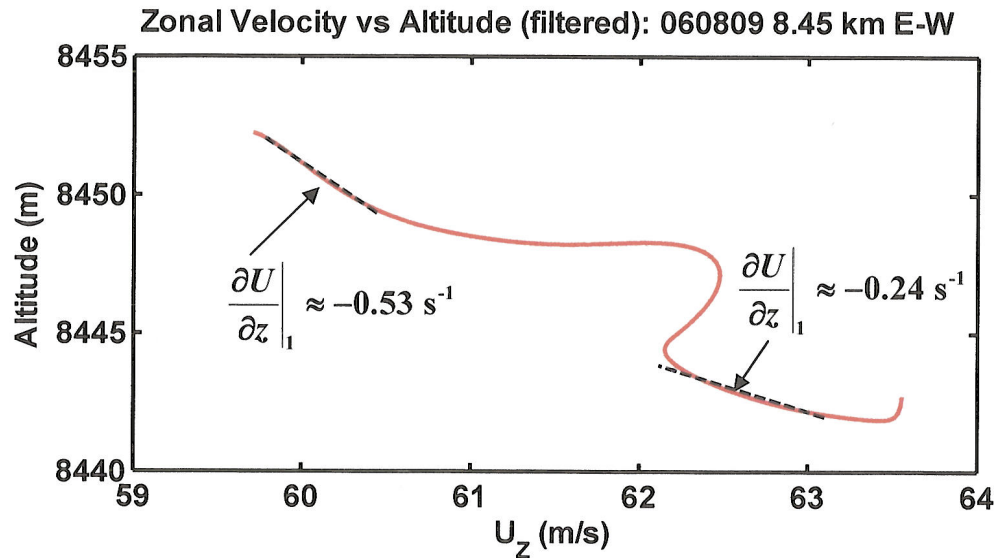
$$R_{w\theta}=0.21, R_{uw}=0.13$$

WHY ARE $\langle W\theta \rangle$ & $\langle uw \rangle$ POSITIVE? EXPLANATION 1



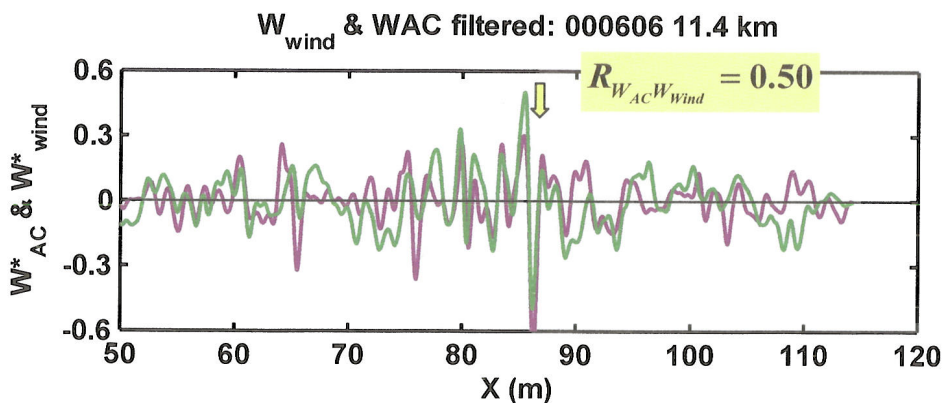
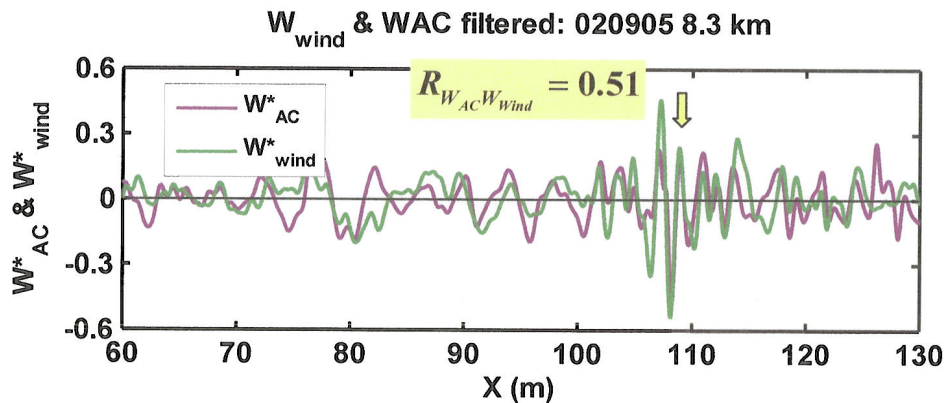
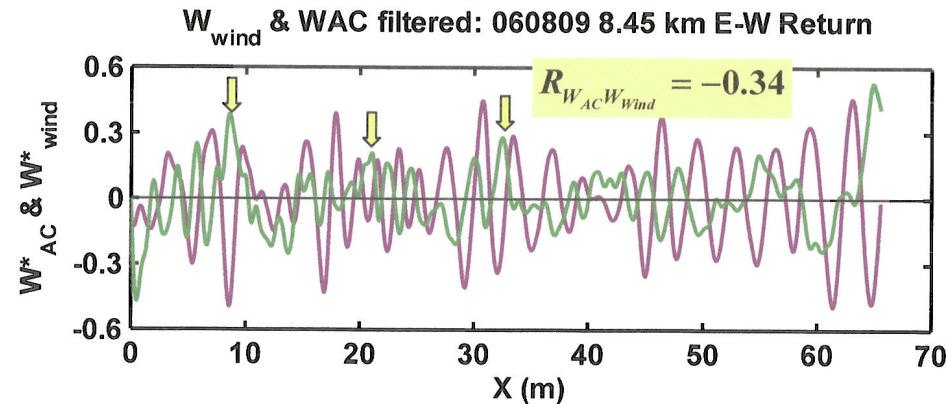
- One possible explanation is that the temperature profile is unstable and shear is negative, but climb profiles don't capture this.
- Though unlikely, it is partly supported by data near the end of 8.45 km segment, when the aircraft is retracing its flight path from East to West (red star in plot)
- During this segment increasing altitude corresponds to decreasing θ and U . See next slide for calculation of vertical gradients based on low-pass filtered data (10 km cutoff)
- Data also show weak cliff ramps (yellow arrow), discussed in slide 26.

WHY ARE $\langle W\theta \rangle$ & $\langle uw \rangle$ POSITIVE? EXPLANATION 1



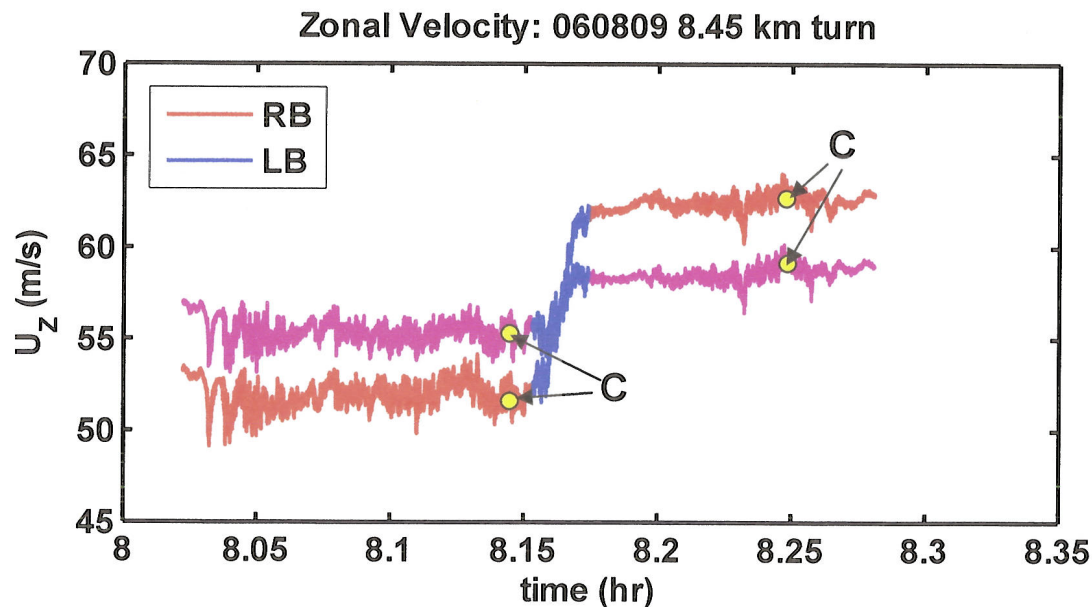
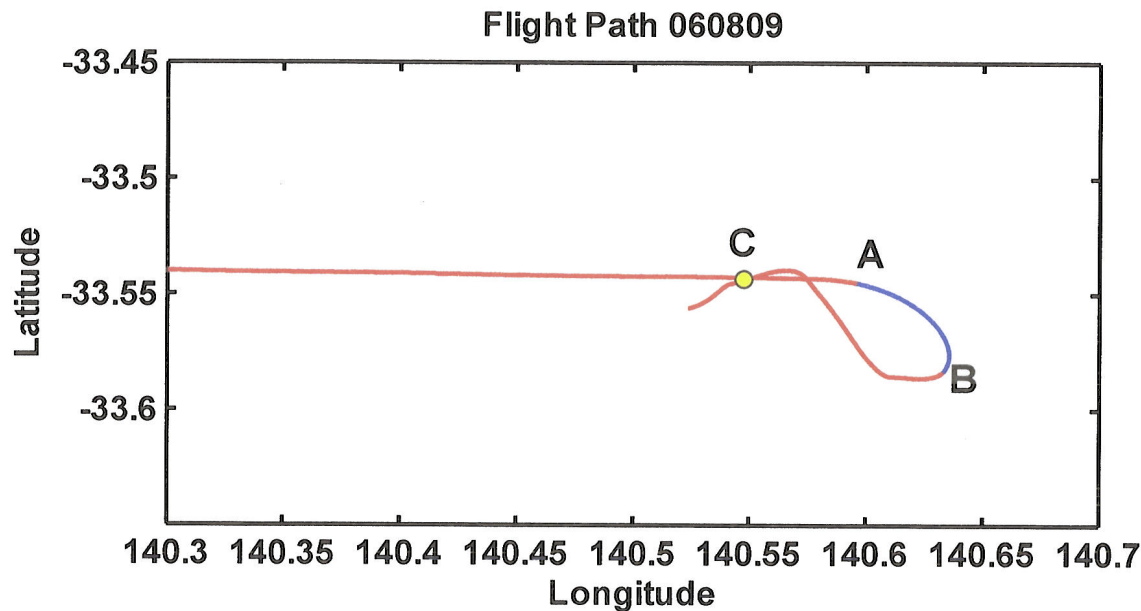
- The vertical profiles of velocity and temperature are not monotonically decreasing. In addition, the estimated gradients are higher than expected.
- These two facts suggest that the changes in velocity and temperature are due to horizontal gradients rather than vertical gradients.
- However, if they are due to vertical gradients, then this is a very unique case, because of the unusual combination of negative shear in a buoyantly unstable region in the upper troposphere.

WHY ARE $\langle W\theta \rangle$ & $\langle uw \rangle$ POSITIVE? EXPLANATION 2



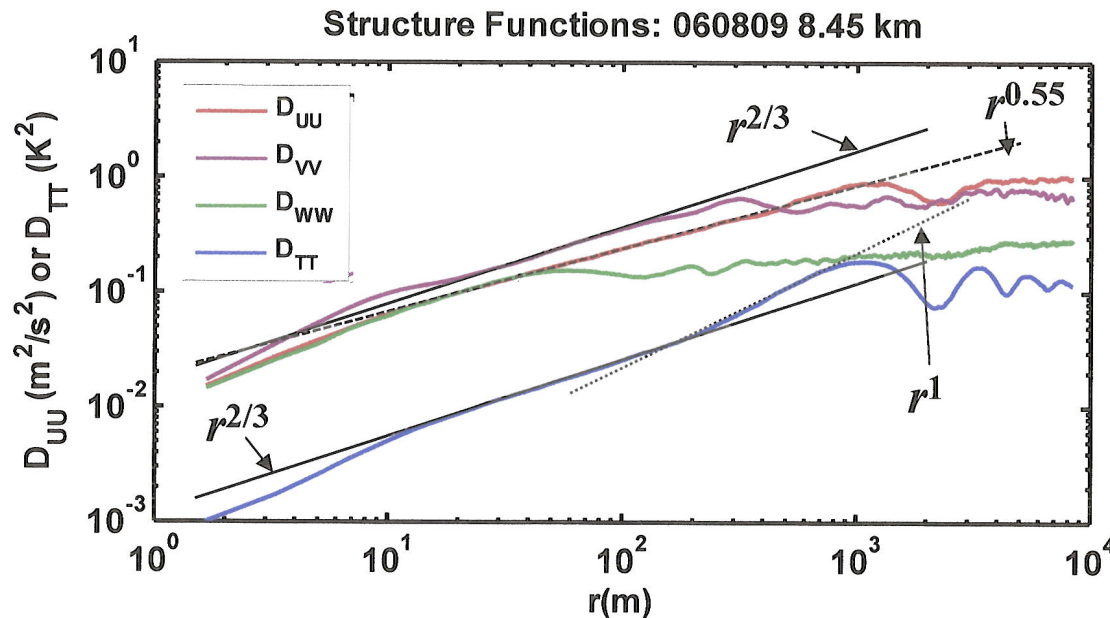
- Another possible explanation is that the temperature profile is stable and shear is positive, but there is a negative sign error in W (possibly introduced in the data reduction)
- To check, look at correlation between wind and aircraft vertical velocities during altitude oscillations, as shown in the figures for the 060809 case and two other CR cases. (NOTE: data is bandpass filtered data, 1 to 20 km, and normalized).
- For 060809, there are several times when the wind and aircraft vertical velocities are 180° out of phase (yellow arrows), which is counterintuitive. For the other two cases, the opposite is true. This is reflected in the correlation coefficients (shown on the graph), which are negative for the 060809 case and positive for the other two cases.
- This suggests that there may be a sign error in vertical velocity data.

ANOTHER POSSIBLE DATA ANOMALY



- The zonal velocity from the left BAT probe (LB) shows a sharp increase from around 52 m/s to 62 m/s during the beginning of the turnaround (from A to B as marked in blue on the plots). A similar but smaller increase is seen in the U_z from the right BAT probe (RB).
- The aircraft then retraces its path in the E-W direction, passing through point C that it passed through during the W-E segment at the same altitude (8,444 m in the W-E pass and 8,446 m in the E-W pass).
- But the velocities don't return to the values seen at point C during the W-E pass.
- This leads to the speculation that there is some data anomaly that occurs during the turn.

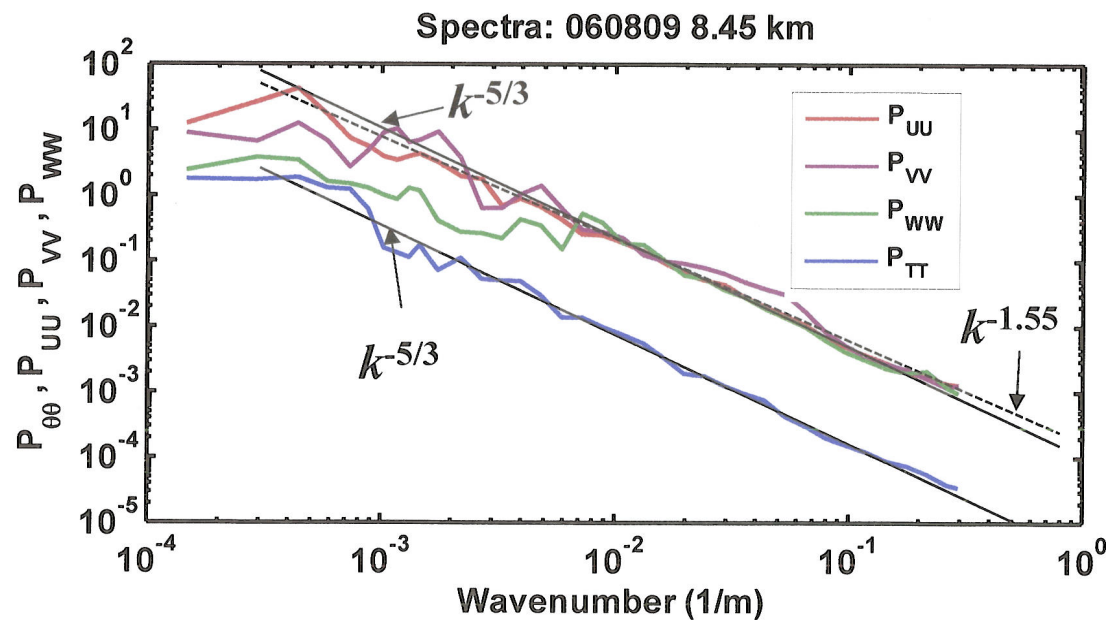
STRUCTURE FUNCTIONS AND SPECTRA: ALL ZONES



- D_{TT} shows clear $r^{2/3}$ inertial range (black solid line), and r^1 region (dotted line). Large scale structure seen in oscillatory behavior for $r > 1000$ m, with wavelength of ≈ 2 km.

- D_{VV} also exhibits an $r^{2/3}$ inertial range, and slight “bump” at $r = 10$ m (also seen in spectra at $k = 0.6 \text{ m}^{-1}$) But D_{UU} and D_{WW} are better fit with an $r^{0.55}$ curve (dashed line) from 10 to 1000 m.

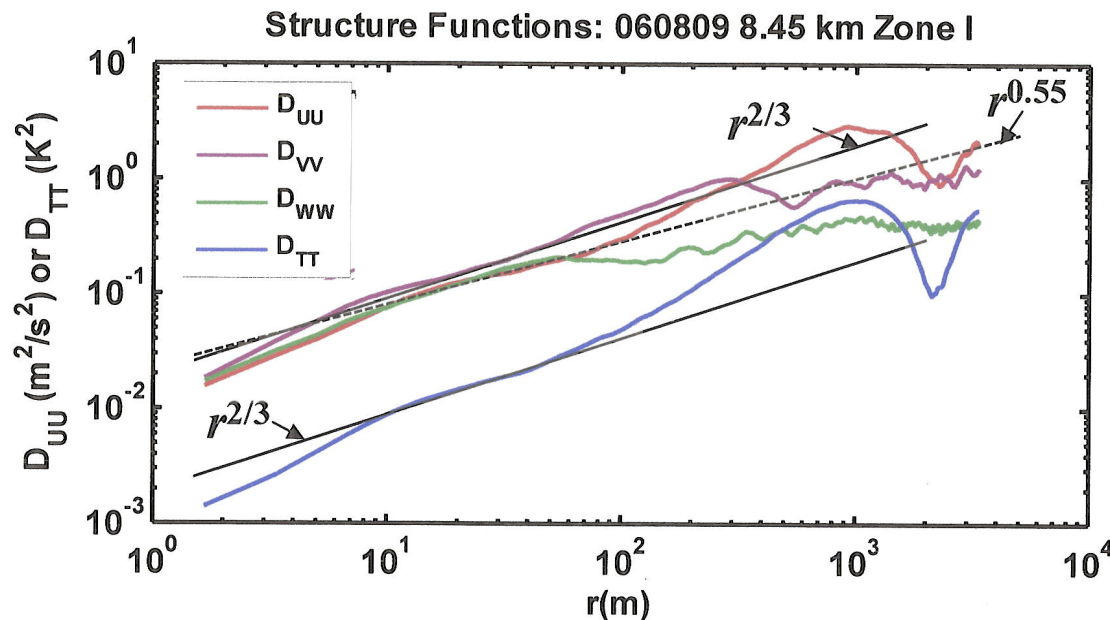
- Temperature spectra consistent with D_{TT} , with $k^{-5/3}$ inertial range.



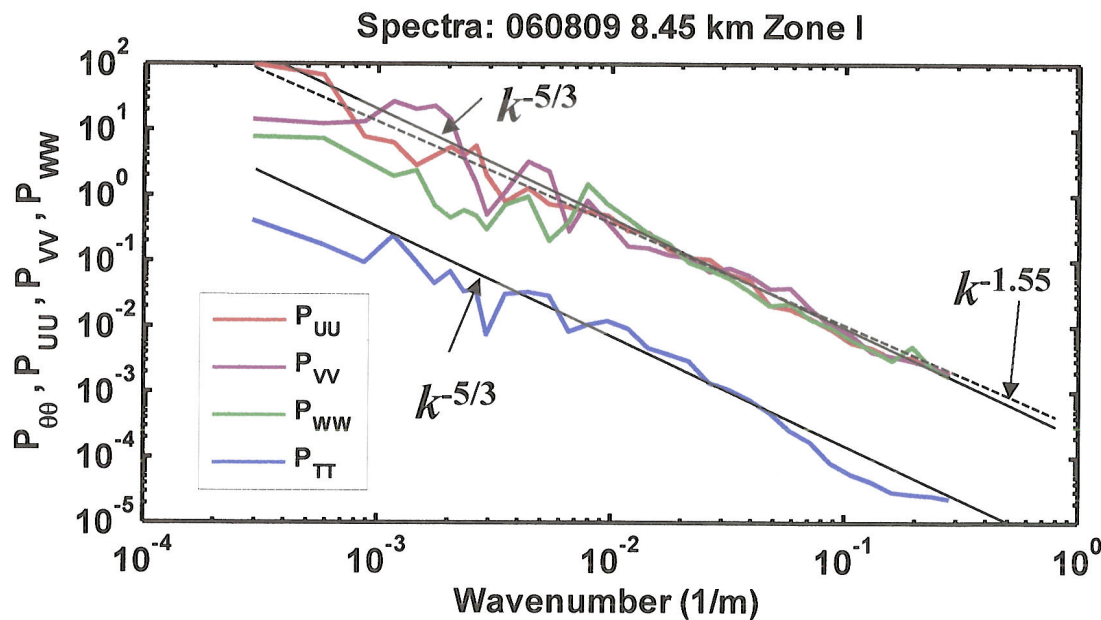
- At first glance, spectra for U seems to exhibit $k^{-5/3}$ behavior, but is better fit with a $k^{-1.55}$ curve, consistent with $r^{0.55}$ behavior seen in structure functions.

- P_{VV} and P_{UU} have small peaks at wavenumber of 0.0005 (2 km)- large scale structures?– but not P_{TT} .

STRUCTURE FUNCTIONS AND SPECTRA: ZONE I

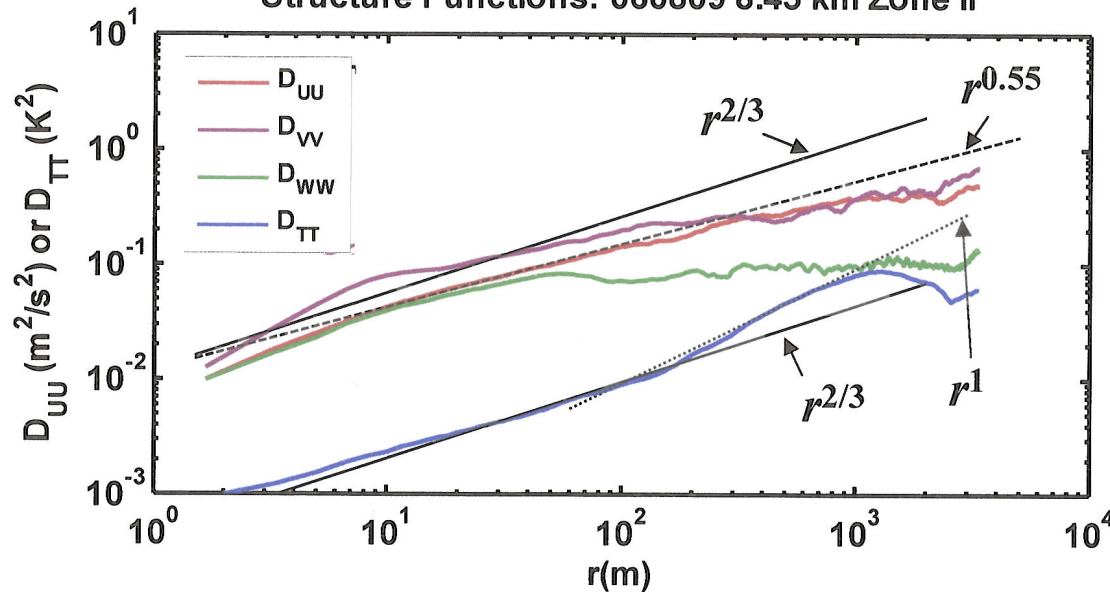


- D_{TT} has inertial range but no r^1 region like D_{TT} for All Zones
- D_{VV} , D_{UU} and D_{WW} all similar to structure functions for All Zones, but $r^{0.55}$ region is shorter (10 to 100 m).
- “Bump” in D_{VV} not as large.
- Spectra not as smooth as those for all zones- not surprising due to smaller sample size-- but behavior is similar.
- Peaks associated with large-scale motions are not seen in spectra because window size for fft's is too small to capture large scale motions.



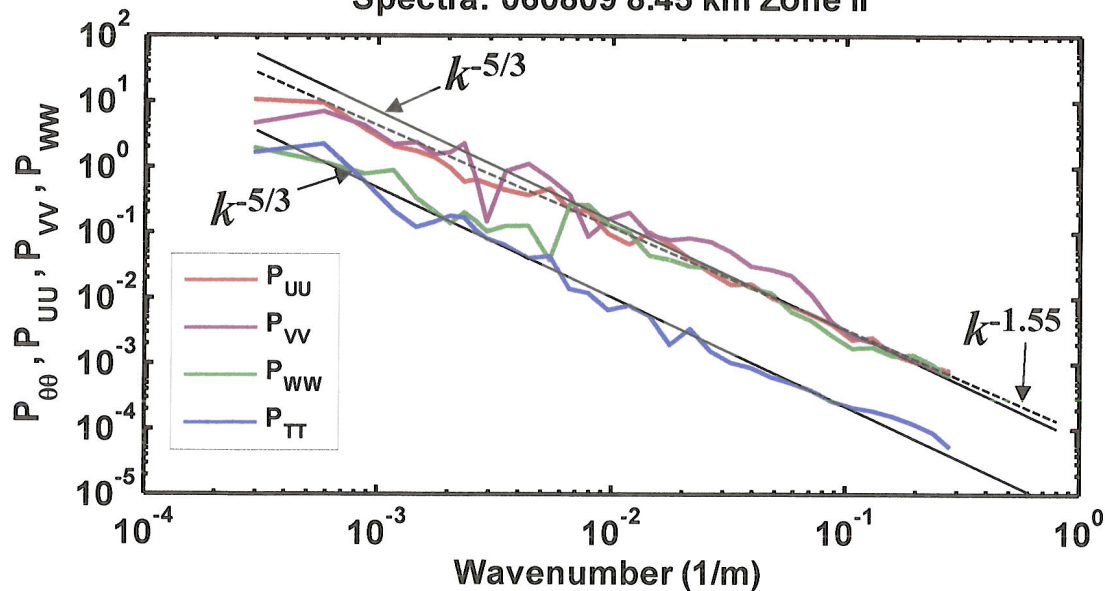
STRUCTURE FUNCTIONS AND SPECTRA: ZONE II

Structure Functions: 060809 8.45 km Zone II

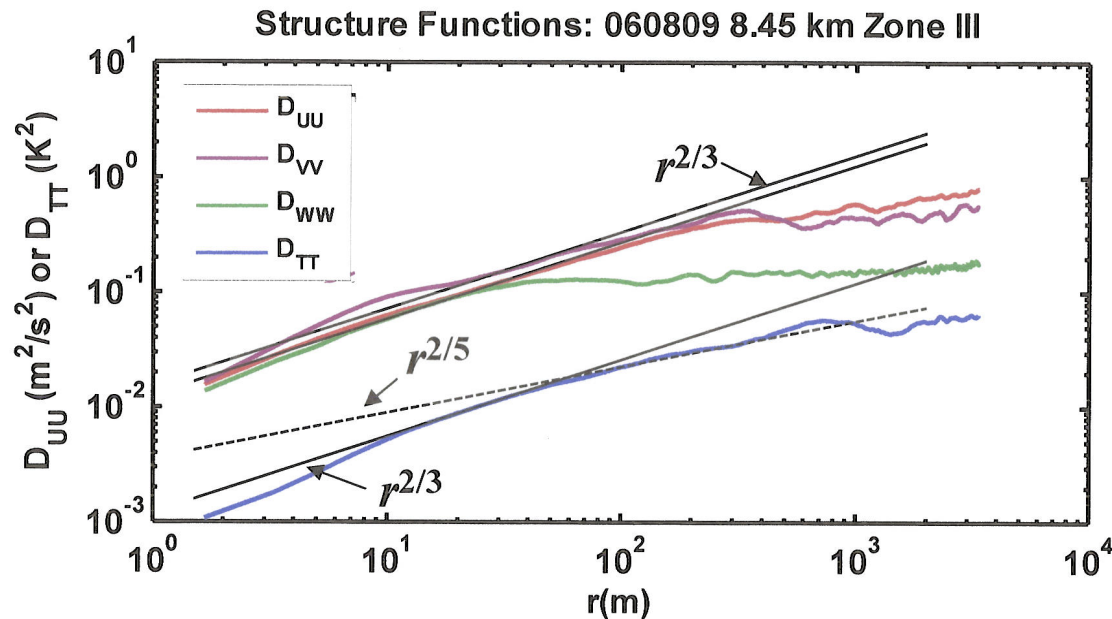


- All structure functions (velocity and temperature) exhibit same functional dependency as those for all zones for $r < 100$, but behavior is different at higher values or r .
- “Bumps” in D_{VV} at $r = 10$ m and in P_{VV} at $k = 0.6 \text{ m}^{-1}$ are more pronounced
- Spectra show similar functional dependencies as those for all zones.

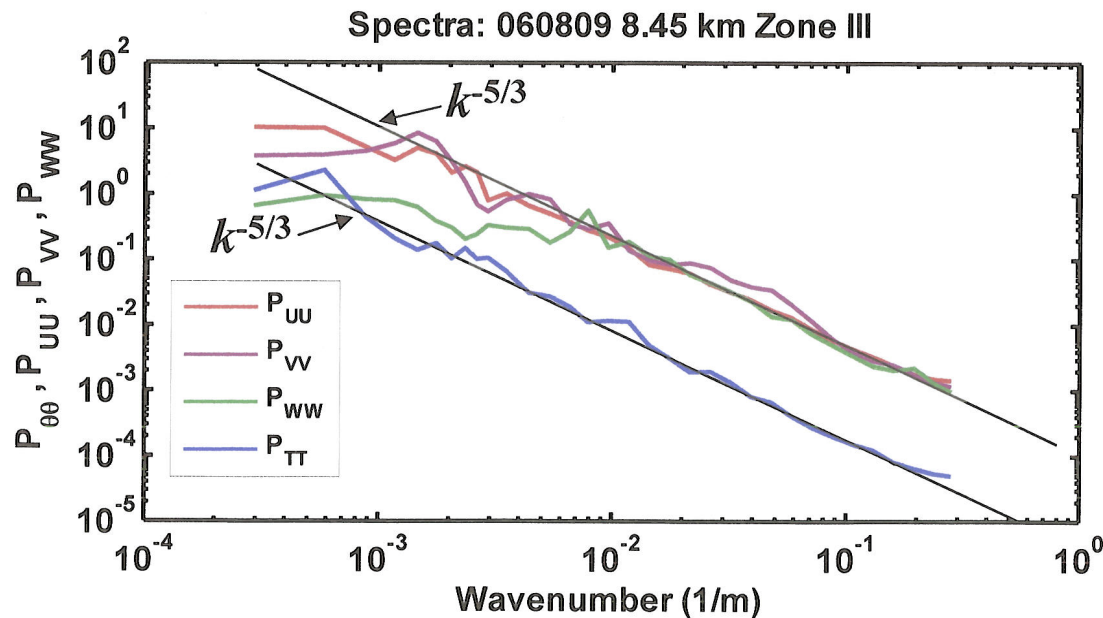
Spectra: 060809 8.45 km Zone II



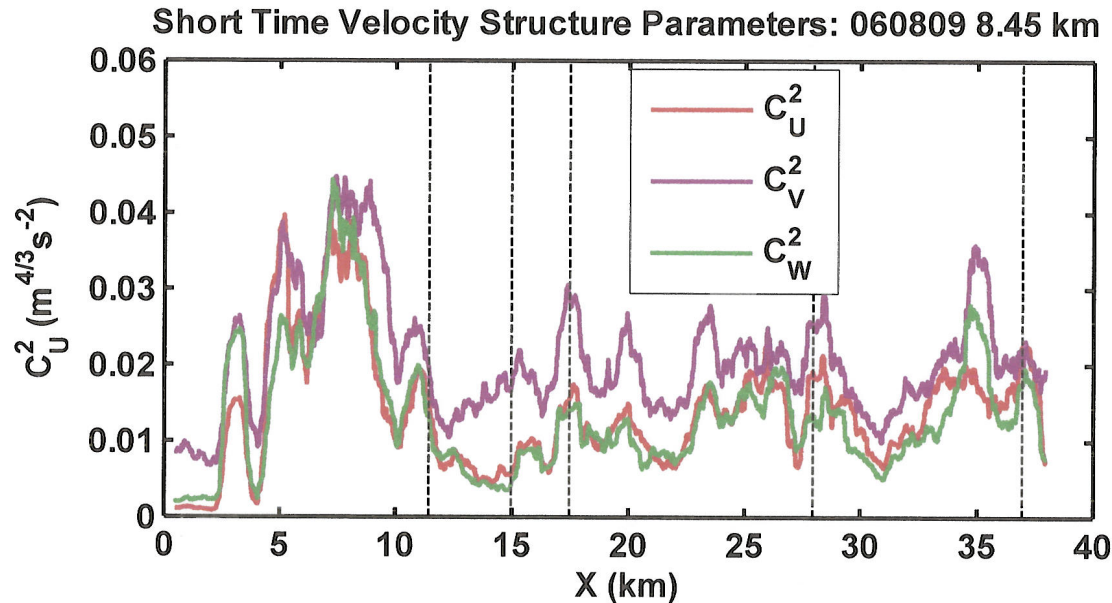
STRUCTURE FUNCTIONS AND SPECTRA: ZONE III



- D_{TT} has $r^{2/5}$ region (dashed line) in addition to $r^{2/3}$ inertial range (black solid line), but corresponding $k^{-7/5}$ is not evident in P_{TT} .
- Large scale motions not evident in the D_{TT} .
- D_{UU} also shows $r^{2/3}$ region and spectra is better fit with $k^{-5/3}$.



SHORT TIME VELOCITY STRUCTURE PARAMETERS



$$EDR = \varepsilon^{1/3} = \sqrt{\frac{C_U^2}{2}}$$

Eddy Dissipation Rate (EDR), based on maximum value of short time C_U^2 in each zone

Zone	I	II	III
EDR	0.11	0.10	0.14

So, these are on low end of the “mild” turbulence range (EDR from 0.1 to 0.25)

- Obtained from short time structure functions for 10 m separation distance, over a sliding 1 km window.
- Plot confirms observation of raw signals that turbulence is highest in Zone I; in particular, the peak turbulence is towards the end of Zone I where the finger-like patterns have given way to symmetric ramps.
- From the point of peak turbulence in Zone I (around 8 km) through to the end of Zone III, C_{UU} and C_{WW} are nearly the same and C_{VV} is consistently higher.

TURBULENCE PARAMETERS & LENGTH SCALES

	Zone I	Zone II	Zone III	ALL
C_T^2 (K ² m ⁻³)	1.91·10 ⁻³	4.43·10 ⁻⁴	1.20·10 ⁻³	1.21·10 ⁻³
C_U^2 (m ^{4/3} s ⁻²)	1.5·310 ⁻²	9.13·10 ⁻³	1.27·10 ⁻²	1.38·10 ⁻²
C_V^2 (m ^{4/3} s ⁻²)	1.96·10 ⁻²	1.22·10 ⁻²	1.55·10 ⁻²	1.71·10 ⁻²
C_W^2 (m ^{4/3} s ⁻²)	1.6710 ⁻²	8.50·10 ⁻³	1.15·10 ⁻²	1.39·10 ⁻²
C_U^2 / C_T^2	8.01	20.6	10.5	11.4
C_V^2 / C_U^2	1.28	1.33	1.23	1.24
C_W^2 / C_U^2	1.09	0.936	0.910	0.971
ε (m ² s ⁻³)	6.76·10 ⁻⁴	3.08·10 ⁻⁴	5.04·10 ⁻⁴	5.73·10 ⁻⁴
ε_V (m ² s ⁻³)	6.30·10 ⁻⁴	3.09·10 ⁻⁴	4.44·10 ⁻⁴	5.14·10 ⁻⁴
ε_W (m ² s ⁻³)	5.00·10 ⁻⁴	1.81·10 ⁻⁴	2.84·10 ⁻⁴	3.56·10 ⁻⁴
σ_W (m s ⁻¹)	0.441	0.303	0.335	0.373
σ_θ (K ²)	0.400	0.192	0.176	0.274
L_E (m)	39.8	19.2	17.6	27.4
L_O (m)	10.7	7.27	9.30	9.91
L_O/L_E	0.27	0.38	0.53	0.36
L_B (m)	24.5	16.8	18.6	20.6
L_{DW} (m)	127.6	90.2	74.7	90.3
L_{DW}/L_B	5.3	5.4	4.0	4.4
L_E/L_B	1.6	1.1	0.95	1.3

Definitions

$$L_E = \frac{\sigma_\theta}{\frac{\partial \Theta}{\partial z}} \quad L_O = \sqrt{\frac{\varepsilon}{N^3}}$$

$$L_B \approx \frac{\sigma_W}{N} \quad L_{DW} \approx \frac{\sigma_W^3}{\varepsilon}$$

$$\varepsilon = \left(\frac{C_U^2}{2} \right)^{1.5} \quad \varepsilon_V = \left(\frac{3C_V^2}{8} \right)^{1.5}$$

$$\varepsilon_W = \left(\frac{3C_W^2}{8} \right)^{1.5}$$

See next slide for
comments

TURBULENCE PARAMETERS & LENGTH SCALES

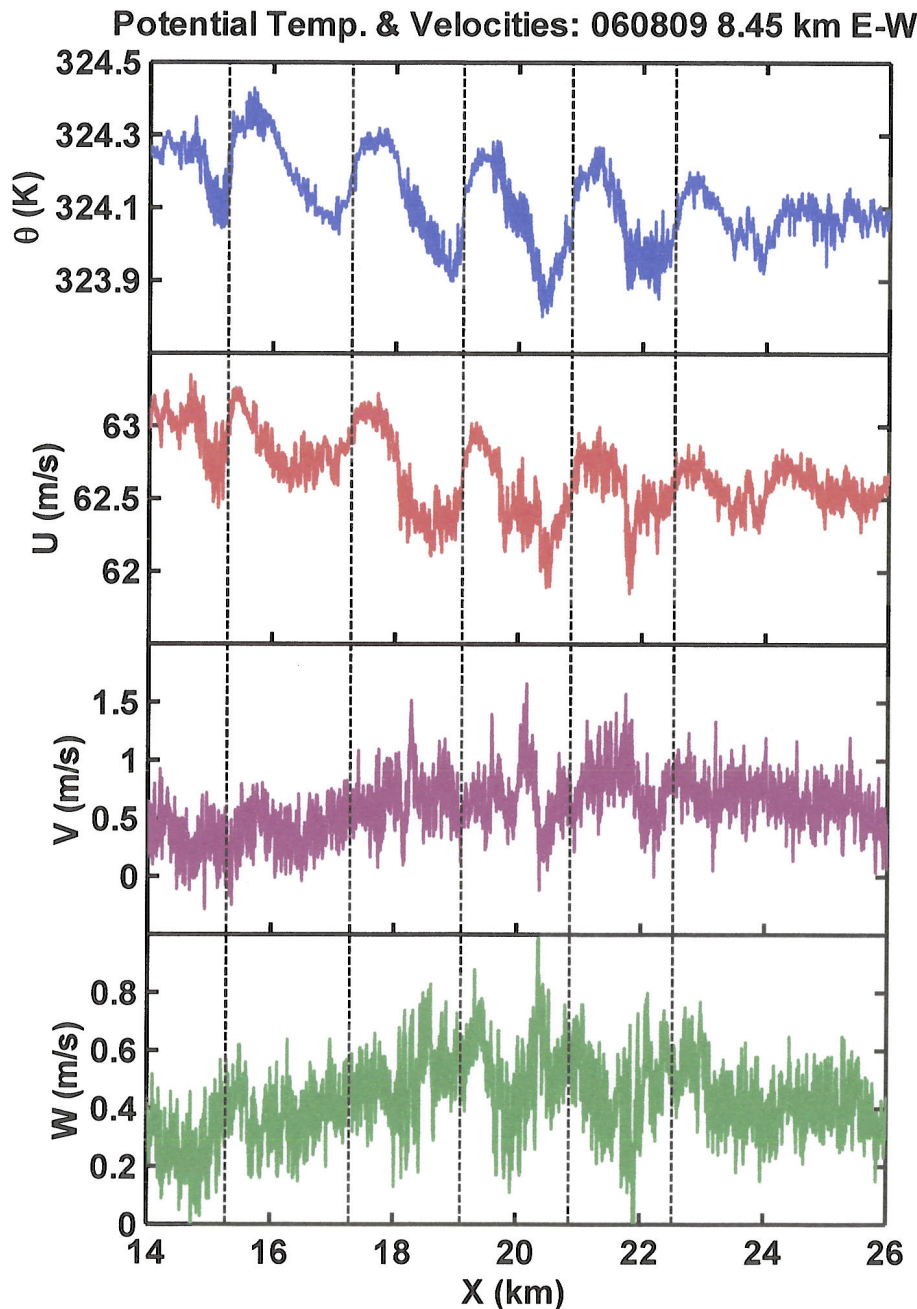
COMMENTS ON PREVIOUS SLIDE

- Structure parameters support observation that the turbulence is highest in Zone I, lowest in Zone II, and intermediate in Zone III.
- Ratio of structure parameters indicate horizontal isotropy (C_v^2 / C_u^2) but vertical anisotropy (C_w^2 / C_u^2).
- Smith and Moum (2000) showed that L_O / L_E ratio increases during the development of a Kelvin Helmholtz layer. (See 2005 Briefing 2). The increasing values of this ratio from Zone I through Zone III suggest that we may be observing a Kelvin-Helmholtz billow developing as we fly through it. This seems like it might be the case for Zone II and Zone III, but the behavior in Zone I seems inconsistent with KH billows in the “roll-up” phase, for two reasons:
 - The large-scale patterns don’t appear to resemble young KH billows
 - Wouldn’t expect highest turbulence to in young KH billows.

Need to check this with J. Werne’s DNS.

- L_{DW} / L_B ratio is much larger than those for other CR/RCs (See slides 3-5, 2006 Briefing 1) which show values close to 1. L_E / L_B ratio are consistent with other CR/RCs, which show values between 1 and 2.5. This suggest L_{DW} values are unusually high for this case. Why?

CLIFF-RAMPS SEEN IN E-W RETURN SEGMENT (E-W CRs)

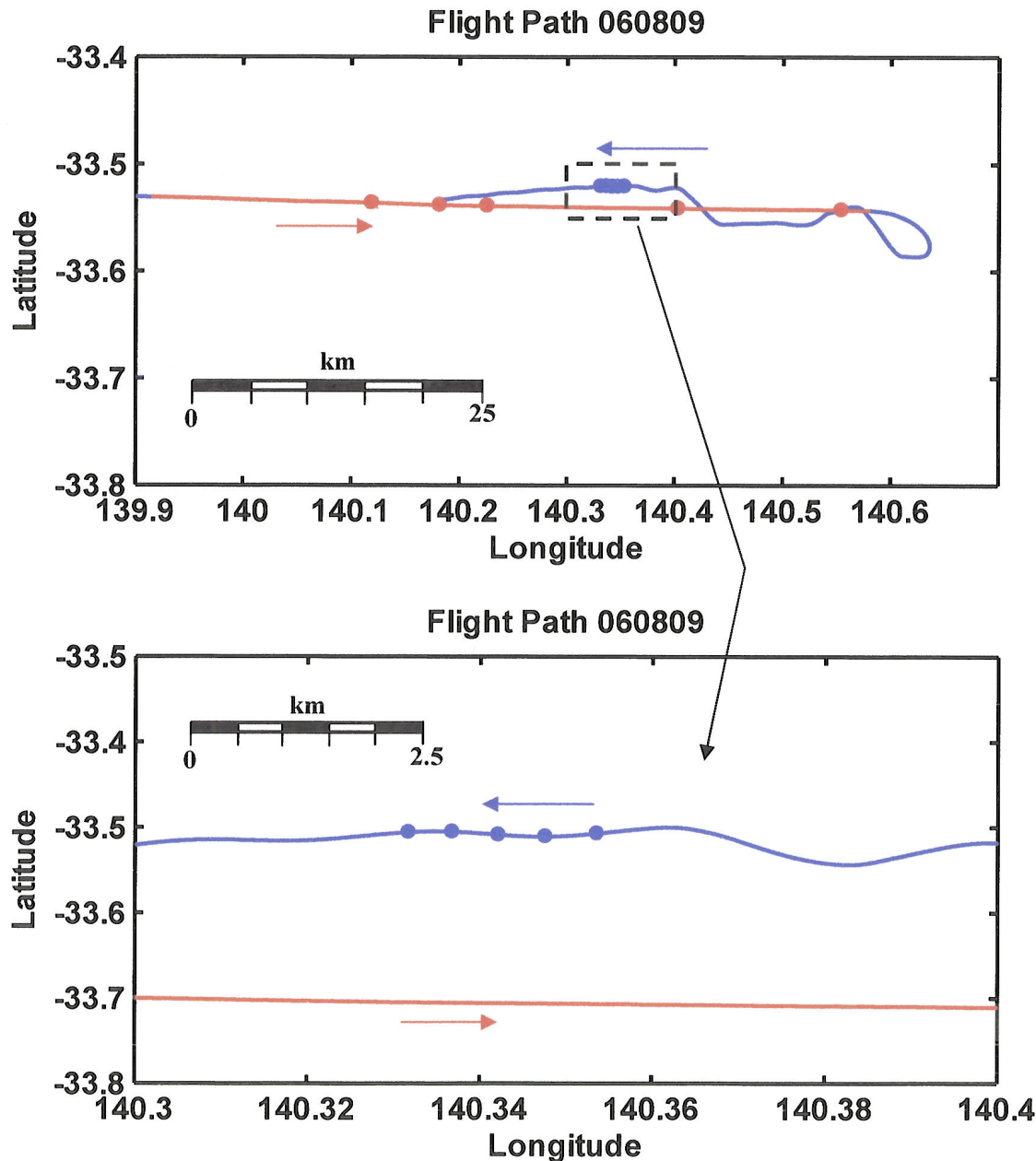


- 5 cliff ramps (CR consistent with headwind and positive shear).

	Cliff width (m)	Wavelength (km)	$\Delta\theta$ (K)	
1.	105	1.74	0.31	
2.	446	1.92	0.25	
3.	428	1.48	0.35	
4.	606	1.99	0.39	
5.	262	1.58	0.21	
AVE 370				1.74
AVE* 145				1.69
				0.30 (E-W CR's)
				0.63 (W-E RC's)

- The **CR's seen in the W-E segment (E-W CR)** have nearly the same average wavelength (in wind relative distance) as the **RC's seen in the W-E segment (W-E RC's)**. But, they have weaker cliffs: i.e., smaller $\Delta\theta$ and less steep cliffs (more symmetric structures)

E-W CR's LOCATION RELATIVE TO W-E RC's

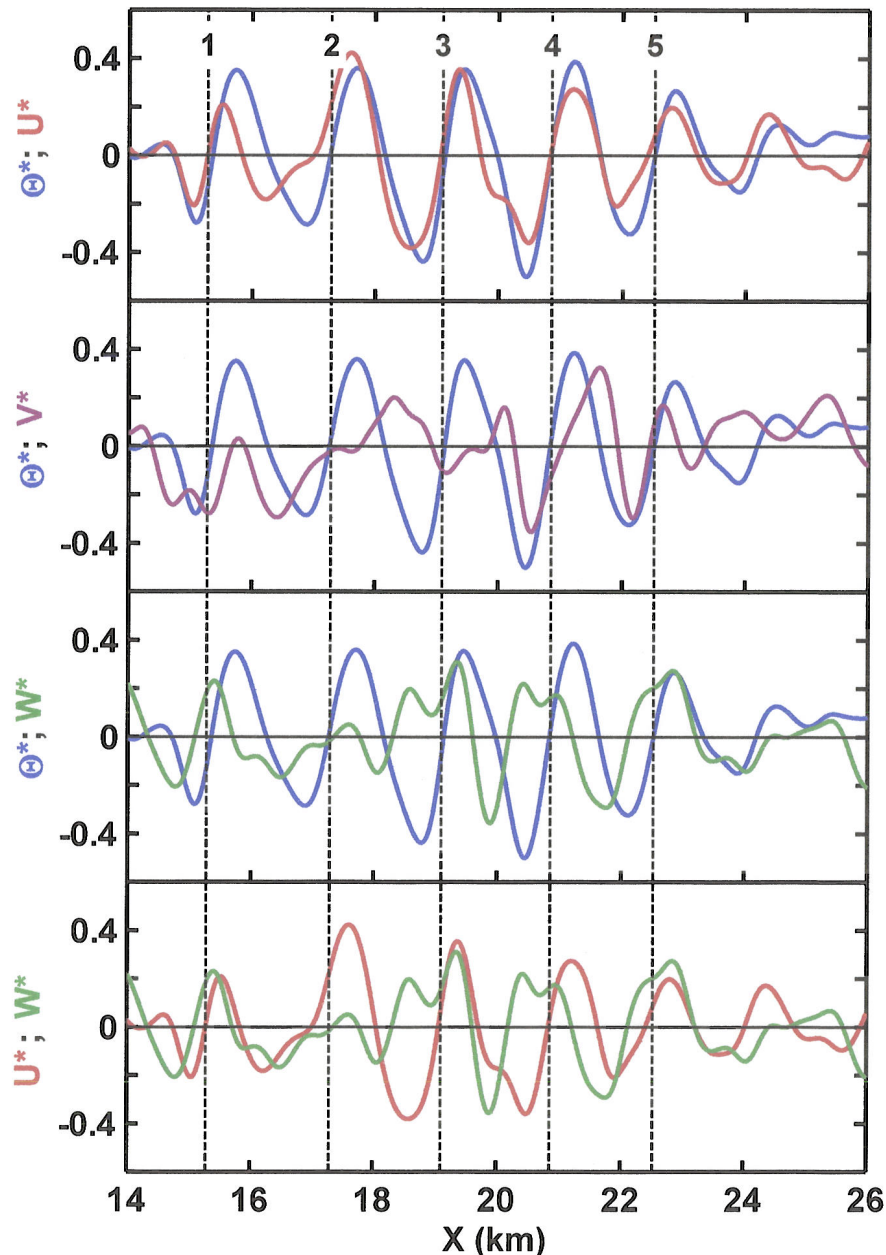


- E-W CR's are in the same general area as the E-W CR's. Note that they are NOT the same structures, which presumably have convected with the mean wind. If they were the same structures, then two sets of CR/RCs should have the same wavelength in ground coordinates, but the opposite is true-- the wavelengths of the are essentially the same in wind relative distance, but clearly substantially different in ground distance as seen in the spacing between adjacent cliffs on the lat-lon plot.

- Since the CRs must develop over a period of time that is probably longer than the time it took to return to the same ground location, it seems likely that the similar locations of the two sets of CRs/RCs is coincidental. But this is still speculative.

FILTERED & NORMALIZED TEMP. & VELOCITIES: E-W CRs

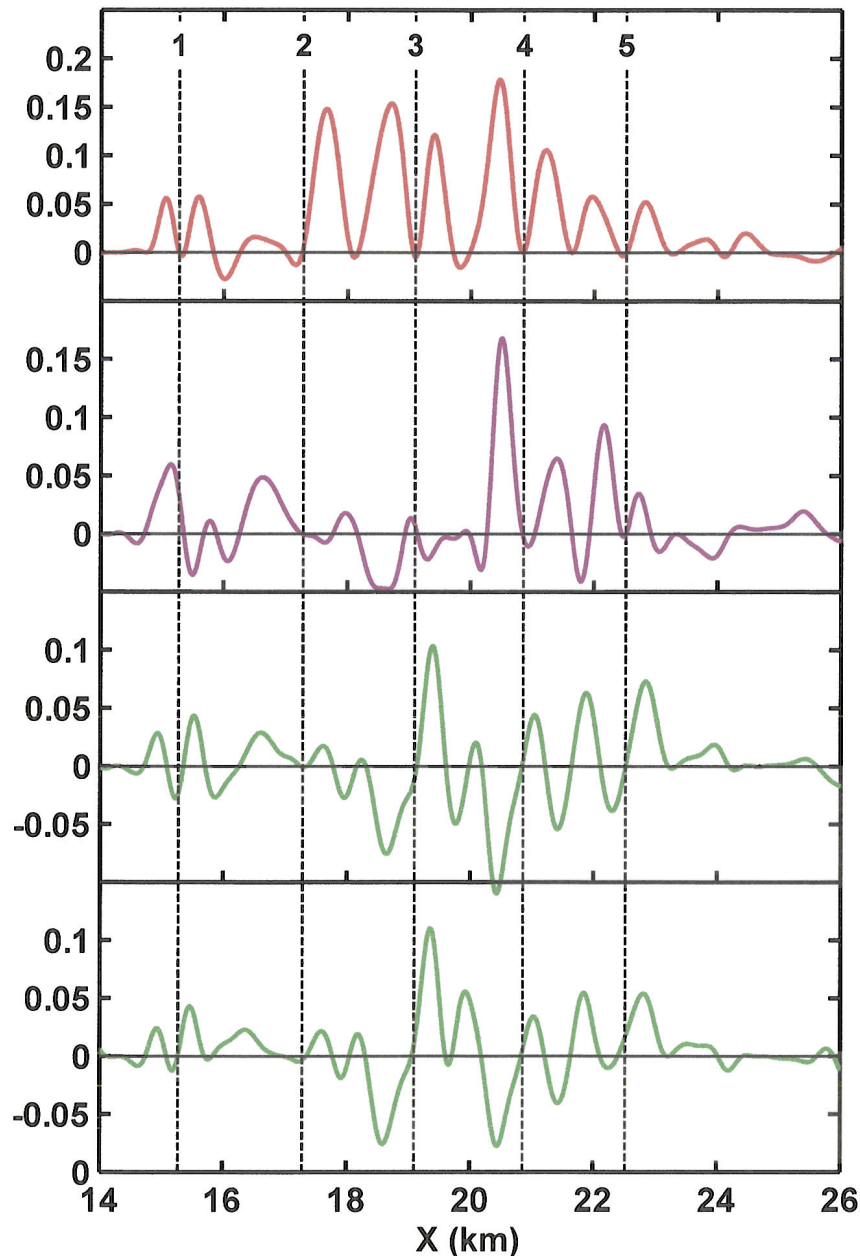
Normalized Filtered U, V, W, θ : 060809 8.45 km E-W



- Velocity and temperature bandpass filtered with a pass band of 0.5 km to 10 km. Filtered signals were then normalized to provide non-dimensional functions with similar amplitudes.
 $X^*=x/\Delta X^*$: $\Delta\theta^*=0.4$ K, $\Delta U^*=0.9$ m/s, $\Delta V^*=0.7$ m/s, $\Delta W^*=0.4$ m/s.
- Like W-E CR's (see slides 13-14), E-W CR's show a close correlation between θ^* and U^* . However, there seems to be a better correlation between V^* and θ^* , like the W-E CR's in Zone III (slide 14).
- W^* correlates well with U^* and θ^* near cliffs 1, 4 and 5, generally increasing with a zero crossing preceding the cliffs.

FILTERED & NORMALIZED FLUXES: E-W CR's

Non-dimensional, Filtered Fluxes: 060809 8.45 km E-W



Correlation Coefficients

$$R_{X^*Y^*} = \frac{\langle X^*Y^* \rangle}{\sigma_{X^*}\sigma_{Y^*}}$$

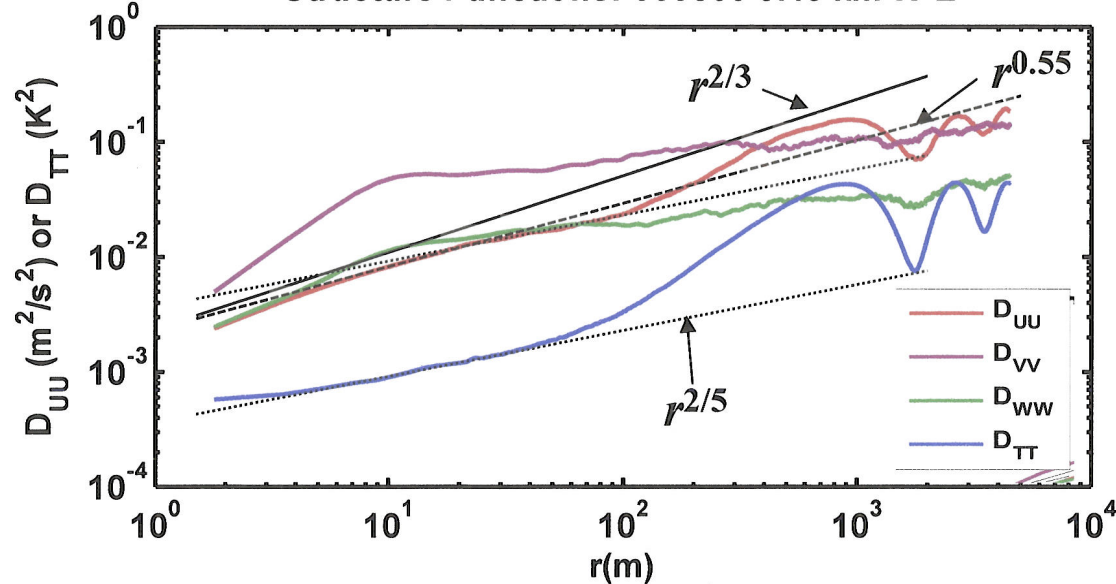
	$R_{U^*\Theta^*}$	$R_{V^*\Theta^*}$	$R_{W^*\Theta^*}$	$R_{U^*\Omega^*}$
E-W CR	0.801	0.270	0.000	0.173
W-E RC *	0.813	0.042	0.624	0.576

* See slide 15

- For **E-W CR's**, $U^*\Theta^* > 0$ for almost the entire time, with correlation coefficients similar to **W-E RC's**
- $V^*\Theta^*$ mostly positive for CR's 4 and 5.
- $W^*\Theta^*$ oscillates between positive and negative with a near zero correlation coefficient. Similar behavior for U^*W^* , but with a non-zero positive correlation coefficient.
- Positive U^*W^* is similar to **W-E RC's** – inconsistent with positive shear.

STRUCTURE FUNCTIONS AND SPECTRA: E-W CR's

Structure Functions: 060809 8.45 km W-E



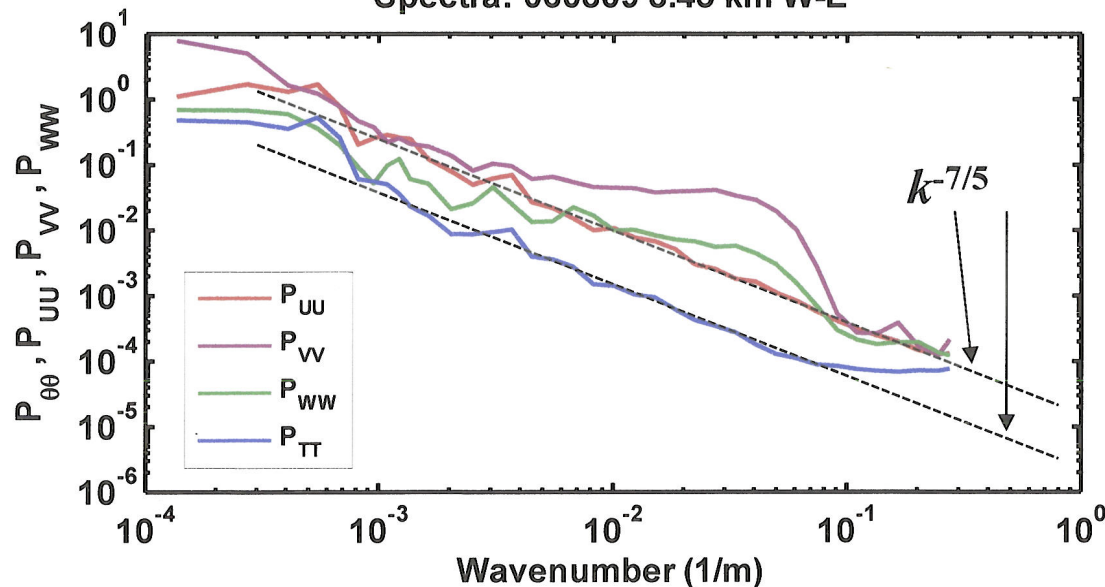
- None of the structure functions show a distinct $r^{2/3}$ inertial range (black solid line).

- D_{TT} has an $r^{2/5}$ region (dotted line). Large scale structure seen in oscillatory behavior for $r > 1000$ m, with wavelength of ≈ 1.8 km.

- D_{UU} shows $r^{0.55}$ in a range small range from 5 to 25 m, and an $r^{2/5}$ region from 25 to 100 m.

- None of the spectra display a $k^{-5/3}$ inertial range. P_{TT} and P_{UU} are best fit by a $k^{-7/5}$ range over a wide range of scales (20 to 1000 m for D_{TT} and 5 to 1000 m for D_{UU} .)

Spectra: 060809 8.45 km W-E



TURBULENCE PARAMETERS & LENGTH SCALES: E-W CRs

	E-W CR	W-E CR			
	ALL	Zone I	Zone II	Zone III	ALL
C_T^2 ($K^2 m^{-23}$)	1.86·10⁻⁴	1.91·10 ⁻³	4.43·10 ⁻⁴	1.20·10 ⁻³	1.21·10 ⁻³
C_U^2 ($m^4/3 s^{-2}$)	1.76·10⁻³	1.5·10 ⁻²	9.13·10 ⁻³	1.27·10 ⁻²	1.38·10 ⁻²
C_U^2 / C_T^2	9.44	8.01	20.6	10.5	11.4
ε ($m^2 s^{-3}$)	2.61·10⁻⁵	6.76·10 ⁻⁴	3.08·10 ⁻⁴	5.04·10 ⁻⁴	5.73·10 ⁻⁴
σ_W ($m s^{-1}$)	0.135	0.441	0.303	0.335	0.373
σ_θ (K^2)	0.118	0.400	0.192	0.176	0.274
L_E (m)	11.8	39.8	19.2	17.6	27.4
L_O (m)	2.1	10.7	7.27	9.30	9.91
L_E/L_O	0.18	0.27	0.38	0.53	0.36
L_B (m)	7.49	24.5	16.8	18.6	20.6
L_{DW} (m)	93.9	127.6	90.2	74.7	90.3
L_{DW}/L_B	12.5	5.3	5.4	4.0	4.4
L_E/L_B	1.6	1.6	1.1	0.95	1.3

• The value of L_O/L_E ratio for the E-W CRs is lower than those seen in the W-E CR's, suggesting that they may be young K-H billows just beginning to form tight braids, and hence observable cliffs. In that sense, they are more likely young K-H billows than the structures seen in Zone I of the W-E CRs.

NOTE: C_V^2 , C_W^2 and associated values are not shown because of the lack of any region in their structure functions with a behavior close to $r^{2/3}$.

SUMMARY

- During the EGRETT flight on 060809, a layer with mild turbulence was observed at an altitude of 8.45 km, approximately 100 to 200 km. downwind of Mt. Lofty range. The layer was about 360 m thick with a Richardson number around 0.2, as seen in both the climb profiles and in the 00Z sounding from Adelaide.
- A series of large-scale structures with wavelengths of 1.5 to 2 km were seen in the temperature and velocity signals measured during the main W-E flight segment. The structures included symmetric features as well as 5 ramp-cliffs (RC). Length scale analysis using L_E/L_O suggested that this layer may have been developing as the aircraft flew through it, transitioning from early K-H “waves” (Zone I), to braided billows with distinct cliff ramps (Zone II), and through to transition when the braids and the cliffs were smoothed by transition to turbulence (Zone III); more work needs to be done to test this theory.
- The RC’s had wavelengths ranging from 1.1 to 2.4 km, with cliff $\Delta\theta$ ranging from 0.47 to 0.87 K. They displayed very close correlations between horizontal wind velocity and temperature, and an unexpected positive correlation between vertical velocity and temperature and horizontal velocity (i.e., positive vertical heat and momentum flux) which was inconsistent with positive shear in a stably stratified region. Analysis of the correlation between aircraft vertical motion and vertical wind suggested that there may be a negative sign error in the vertical velocity that led to this inconsistency— this should be checked out.

SUMMARY

- Structure functions for horizontal velocity showed an $r^{2/3}$ region ($k^{-5/3}$ for spectra) only in Zone III. For Zones I and II, the data was better fit with an $r^{0.55}$ region ($k^{-1.55}$ for spectra).
- The small scale turbulence was strongest during Zone I and weakest during Zone II, when the RC's were seen. This is opposite to what had been observed in previous Cliff-ramp, ramp-cliff cases, when the turbulence was generally highest when the cliff-ramps were observed.
- Length scale analysis revealed that L_{DW}/L_B ratios were much larger than those for other CR/RCs (See slides 3-5, 2006 Briefing 1)— values of 4-5 compared to values close to 1. The L_E/L_B ratios, on the other hand, are consistent with other CR/RCs, which show values between 1 and 2.5. This suggested that L_{DW} values are unusually high for this case— the reason for this needs to be investigated further.
- Smaller, weaker cliff ramps (CR) were seen during the return segment (E-W) at approximately the same location as the E-W RC's. These CR's had approximately the same wavelengths as the W-E RC's, but had weaker, broader cliffs. The structure functions, D_{UU} and D_{TT} both exhibited $r^{2/5}$ behavior, also seen as $k^{-7/5}$ in the spectra. They showed similar correlations between U and θ , but there was little correlation between W and θ (zero vertical heat flux). The L_E/L_O length scale analysis suggested that these were cliff ramps in an earlier stage of development compared to the W-E RCs.